Andreia Sofia da Costa Vieira

Bachelor degree in Biochemistry

Rethinking Triazoles as Antifungals: Synthesis and Evaluation of New Triazole Derivatives

Dissertation for the Master degree in Biochemistry for Health

Supervisor: Ana Petronilho, Auxiliary Investigator, ITQB-NOVA

Co-Supervisor: Catarina Pimentel, Auxiliary Investigator, ITQB-NOVA

October 2017

Andreia Sofia da Costa Vieira

Bachelor degree in Biochemistry

Rethinking Triazoles as Antifungals: Synthesis and Evaluation of New Triazole Derivatives

Dissertation for the Master degree in Biochemistry for Health

Supervisor: Ana Petronilho, Auxiliary Investigator, ITQB-NOVA

Co-Supervisor: Catarina Pimentel, Auxiliary Investigator, ITQB-NOVA

Jury:

President: Doutor Pedro Manuel H. M. Matias, Principal Investigator ITQB-NOVA

Arguer: Doutora Maria Rita Mendes B. Ventura, Auxiliary Investigator ITQB-NOVA

Vowels: Doutora Margarida Archer Franco Frazão, Principal Investigator ITQB-NOVA

Doutora Ana Petronilho, Auxiliary Investigator ITQB-NOVA

Instituto de Tecnologia Química e Biológica António Xavier da Universidade Nova de Lisboa

October 2017

Rethinking Triazoles as Antifungals: Synthesis and Evaluation of New Triazole Derivatives

Acknowledgements

First of all, I would like to acknowledge my supervisors Dr. Ana Petronilho and Dr. Catarina Pimentel not only for the opportunity to allow me to work in a challenging project combining two distinctive areas, such as, but also for the continuous support and availability over the last year.

Also, a word of sincere gratitude to Maria Inês, Soraia Caetano and Catarina Amaral, mainly for their guidance and for always being present to assist me during the laboratory activities.

To my colleagues and friends, for all the companionship along these two fantastic years that we spent together, thank you.

Not less important, I cannot fail to mention my parents, for providing me with all the means, so that I could finish yet another stage of my academic career.

Finally, to Gustavo Marquês, thank you for the never-ending patience and encouragement throughout the years.

Resumo

Na última década, as infeções fúngicas tornaram-se um sério problema, principalmente devido ao excessivo uso de medicamentos antifúngicos, levando ao aumento das resistências adquiridas[1]. Assim sendo, é urgente desenvolver medicamentos antifúngicos mais eficazes.

O objetivo principal deste projeto de mestrado foi o desenvolvimento de novos agentes antifúngicos derivados de triazóis e pirimidinas, combinando numa só molécula dois grupos com atividade antifúngica. Na elaboração destes compostos foram utilizadas metodologias de cicloadição 1,3-dipolar de Huisgen, catalisadas por cobre[2] ou ruténio[3]. Assim, foram sintetizados com sucesso 1,4- e 1,5-triazóis derivados de azidotimidina e correspondentes sais metilados. Foram sintetizados igualmente os 1.4-triazóis derivados de 5-fluorouracilo assim como um derivado metilado. Na sua maioria, os triazóis derivados da azidotimidina apresentaram rendimentos superiores aos do 5-fluorouracilo.

A atividade antifúngica destes compostos foi testada, utilizando como modelos os fungos *Saccharomyces cerevisiae* e *Candida glabrata*. Apenas um composto (**8**) apresentou capacidade de influenciar negativamente o crescimento do fungo *Saccharomyces cerevisiae*. Em relação ao fungo *Candida glabrata* nenhum dos compostos nas concentrações testadas apresentou capacidade de influenciar o crescimento deste fungo.

Adicionalmente, foram estudadas metodologias para a síntese de compostos de fluconazol estabilizados por ferro, bem como para a síntese de carbenos NHC de prata derivados de AZT. A coordenação do fluconazol a ferro foi bem-sucedida, obtendo-se um composto resultante da coordenação a Fe(II) de duas moléculas de fluconazol. Estudos de estabilidade em meio aquoso para este composto mostraram que a coordenação ao centro metálico nestas condições não se mantém, recuperando-se o fluconazol livre. Relativamente à formação de carbenos NHC de prata, o composto **8** reagiu com óxido de prata, com rendimento espectroscópico de 55 %. Tentativas de otimização do rendimento desta reação, e a separação de novo composto, não foram bem-sucedidas.

Palavras-chave: agentes antifúngicos, azóis, pirimidinas, metais de transição, carbenos N-heterociclicos

Abstract

In the last decades, fungal infections have become a serious problem, mainly due to the excessive use of this reduced number of drugs, leading to an increase of acquired resistances[1]. Therefore, it is urgent to develop new and more effective antifungal medicines.

The main objective of this master's thesis was the development of novel antifungal drugs, based on triazoles and pyrimidines, combining two groups with antifungal properties, known to be active in combinatorial therapies, in a single molecule. For the synthesis of these compounds, Huisgen's 1,3-dipolar cycloaddition methodologies, catalyzed by copper[2] or ruthenium[3] were employed. 1,4- and 1,5-triazoles derived from AZT (azidothymidine) were synthesized successfully as well as their methylated triazolium salts. Similarly, 1,4-triazoles derived from 5-fluorouracil were synthesized, as well as one methylated derivative. In general, the synthesis of the azidothymidine derivatives presented higher yields than those of 5-fluorouracil.

The antifungal activity of these compounds was evaluated, using as models the fungi *Saccharomyces cerevisiae* and C*andida glabrata*. Only one compound (**8**) displayed the ability to negatively influence the growth of the fungus *Saccharomyces cerevisiae*. Relatively, to *Candida glabrata* none of the compounds in the tested concentrations had the capacity to influence its growth.

Additionally, methodologies for the synthesis of fluconazole compounds stabilized by iron were studied, as well as synthetic methods for silver NHC carbenes derived from AZT. The coordination of fluconazole to iron was successful, obtaining a compound resulting from the coordination of Fe(II) to two molecules of fluconazole. Stability studies in aqueous solution showed that coordination to the metal center under these conditions is not stable, and free fluconazole can be recovered by crystallization. Concerning the formation of silver NHC carbenes, compound **8** react with silver oxide, but with a spectroscopic yield of 55%. Attempts to optimize the spectroscopic yield of this reaction were not successful.

Keywords: antifungal agents, azoles, pyrimidines, transition metals, N-heterocyclic carbenes

Index

Figure index

Scheme index

Table index

Acronyms list

^{13}C-NMR	Carbon-13 nuclear magnetic resonance
^{1}H-NMR	Proton nuclear magnetic resonance
5-FC	5-fluorocytosine
5-FU	5-fluorouracil
Ar	Aromatic
AZT	3`-azido-3`-deoxythymidine
CuAAC	Copper(I)-catalyzed azide-alkyne cycloaddition
d	Doublet
DCM	Dichloromethane
DMF	Dimethylformamide
DMSO	Dimethyl sulfoxide
DMSO-d_6	Deuterated dimethyl sulfoxide
DNA	Deoxyribonucleic acid
eq.	Equivalent
et al.	*et alia* (from Latin, meaning “and others”)
FdUMP	5-fluorodeoxyuridine monophosphate
Fluc	Fluconazole
FUTP	5-fluorouridine triphosphate
HIV	Human Immunodeficiency Virus
Hz	Hertz
J	Coupling constants
m	Multiplet
MeOH	Methanol
MIC	Minimum inhibitory concentration
m/z	Mass-to-charge ratio
Ph	Phenyl
RNA	Ribonucleic acid RNA
RPMI 1640 medium	Roswell Park Memorial Institute 1640 medium
RuAAC	Ruthenium-catalyzed azide-alkyne cycloaddition
q	Quartet
s	Singlet
SCM	Complete synthetic medium
t	Triplet
Trz	Triazole
v/v	Volume/volume ratio

YPD	Yeast extract peptone dextrose
δ	Chemical shift

1. Introduction

Fungi are a group of microorganisms spanning from unicellular forms (yeasts) to multicellular fungus, such as molds or mushrooms. Due to their metabolic abilities, many fungi play beneficial roles, for instance on the fermentation of bread, on the production of antibiotics, and on the decomposition of dead organisms. However, fungi can be opportunistic pathogens and cause diseases on plants, humans and other animals[4].

During the past decades, fungal infections have become an alarming and serious topic, due to a great increase of fungal diseases and mortality caused by these infections on humans[5]. Pathogenic fungi are the cause of billions of infections annually, with ~1.5 million attributable mortalities, a number comparable to that of tuberculosis and malaria[6]. Yet, the escalation of fungal infections on humans have been largely overlooked[6]. The rise of immunocompromised patients (such as those subject to haematopoietic stem cell transplantation, solid organs transplant, aggressive regimens of chemotherapy and HIV patients)[5,7] led to an increase of fungal infections, while the relative low number of available antifungal agents forced an excessive utilization of these drugs. These factors combined potentiated the development of a large number of resistances against the existing antifungal agents. Most infections are caused by species belonging to four categories of fungi: *Aspergillus*, *Candida*, *Cryptococcus*, and *Pneumocystis*[8], with invasive candidiasis being responsible for the majority of cases in what concerns hospital-acquire blood stem infections[9].

In recent years, no considerable advances were achieved regarding antifungal therapies. Research on novel antifungals is particularly complex, since fungal pathogens are closely related to the host on a cellular level, decreasing the pathogen-specific targets[9], and making difficult to develop broad spectrum compounds. In addition, reduced research funding in this area in recent years is also a major reason responsible for the limited drug development[8].

This chapter will further describe existing antifungal drugs, their modus operandi and multiple antifungal resistances, as well as synthetic methods employed in this research project.

1.1. Currently used Antifungals

Fungal infections are treated by a variety of compounds. At present, *circa* 15 antifungal agents are approved for clinical use, but these drugs present issues regarding potency, safety and pharmacokinetic properties. Current drugs can be classified in four main classes: polyenes (*e.g.* amphotericin B); echinocandins (*e.g.* caspofungin); azole derivatives (*e.g.* fluconazole, ketoconazole, itraconazole, and voriconazole) and pyrimidines (*e.g.* 5-fluorocytosine)[10]. These antifungal drugs have a limited number of target structures, mostly affecting the fungal cell

membrane through disruption of ergosterol, β-1,3-d-glucan, or DNA/RNA synthesis[11] (Figure 1.1).

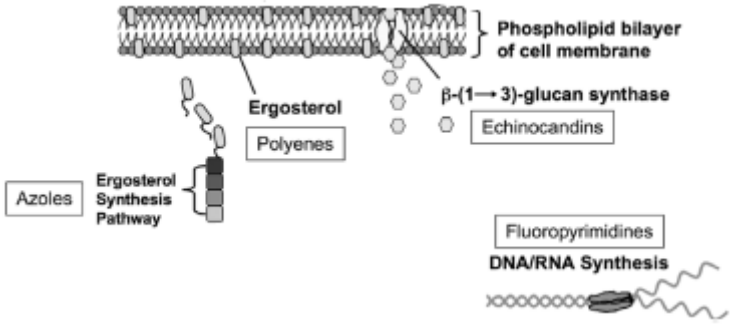

Figure 1.1-Most commonly used antifungal classes and corresponding targets[I].

In the following sections, the modus operandi of these compounds will be briefly discussed, as well as their associated mechanisms of resistance.

1.1.1. Polyenes

Amphotericin B (Figure 1.2) was the first polyene utilized for the treatment of fungal infections, since 1958, and was the most employed antifungal drug until fluconazole approval[12].

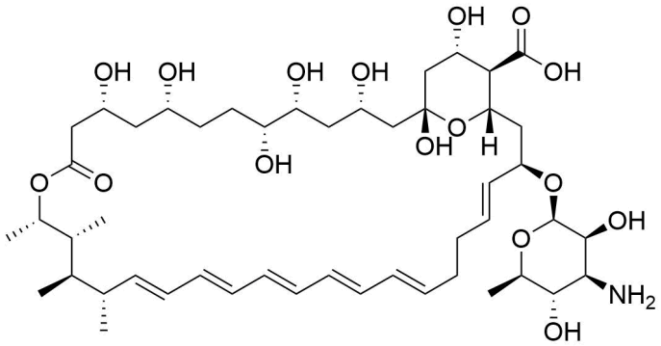

Figure 1.2- Structure of Amphotericin B

The mechanism of action of polyenes, such as Amphotericin B, lies on the stability of the fungal cell. Polyenes bind directly to ergosterol, a sterol found in fungi cell membranes with similar functions to those of cholesterol in animal cells, forming complexes that intercalate with the membrane[12,13] (Figure 1.3), resulting in the formation of pores that lead to an increase in cellular permeability[14], leakage of small molecules[15] and death of the organism[16]. Ergosterol is absent on animals and as such it is a useful target for antifungal drugs[17].

[I]Adapted from Ashley, E. S. D. *et al. (reference 10)*

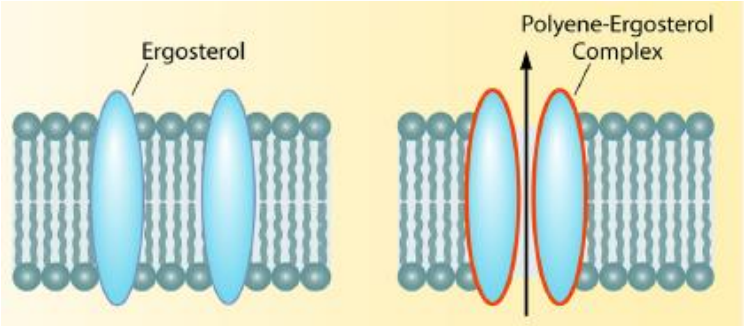

Figure 1.3- Mechanism of action polyenes[II]

1.1.2. Echinocandins

Echinocandins, such as caspofungin (Figure 1.4), are lipopeptide molecules, specifically cyclic hexapeptide with modified N-linked acyl lipid side chains[18]. They exert their antifungal activity by inhibiting the β-1,3-d-glucan synthesis, a fundamental component of the fungal cell wall.

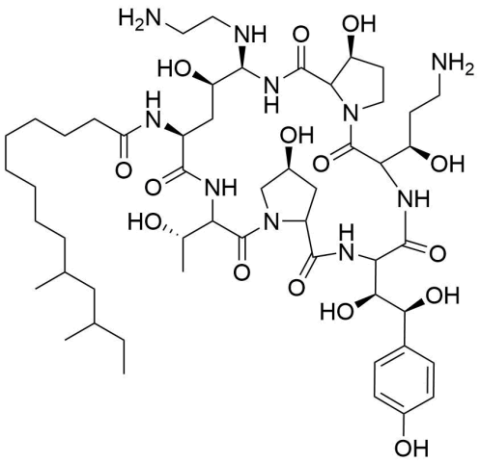

Figure 1.4- Structure of Caspofungin

The disruption of β-1,3-d-glucan synthesis causes osmotic instability and eventually death[14]. Since β-1,3-d-glucan is not present in mammalian cell walls, echinocandins are selective to fungi and present lower toxicity and reduced side effects to the patient[12].

1.1.3. Azoles

Azoles are the most commonly used antifungals. They are constituted by a five-member ring with at least one nitrogen atom. For the azoles currently used as antifungals, the main structures comprise exclusively imidazoles and triazoles, containing two and three nitrogen atoms respectively[19].

[II] Adapted from Shapiro, R. S. *et al. (reference 12)*

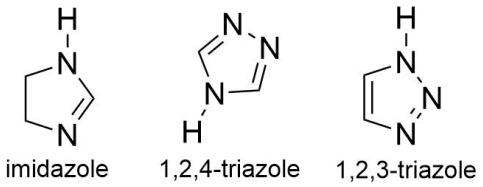

Figure 1.5-Types of azoles: imidazole, 1,2,4-triazole and 1,2,3-triazole

Although the first report of antifungal activity of an azole compound (benzimidazole) was already described in 1944 by Woolley, it was not until the introduction of topical chlormidazole in 1958, that researchers became interested in the antifungal activity of this class of compounds[19]. Fluconazole, a broad-spectrum triazole antifungal developed by Pfizer was approved for use in 1990[11,20]. Fluconazole presents high aqueous solubility, small molecular size, relatively low toxicity, its absorption is not influenced by gastric pH, and it can enter the cerebrospinal fluid extremely well. Fluconazole is generally utilized as first line antifungal therapy for the treatment of candida infections, disseminated candidiasis and cryptococcal meningitis[17,21].

The mechanism of action of azoles targets the ergosterol (ergosta-5,7,22-trien-3β-ol) synthesis[1] (Figure 1.6). Specifically, azoles will bind to the iron of the active site of the enzyme lanosterol 14-α-demethylase, a cytochrome P-450 dependent enzyme, through a nitrogen atom of the azole ring. This process precludes the ergosterol synthesis and promotes the synthesis and accumulation of 14α-methyl-3,6-diol, a toxic sterol. The latter causes increased permeability of the fungal cell membrane, disrupts the enzymes bound to the membrane, and inhibits fungal growth and replication[13,20].

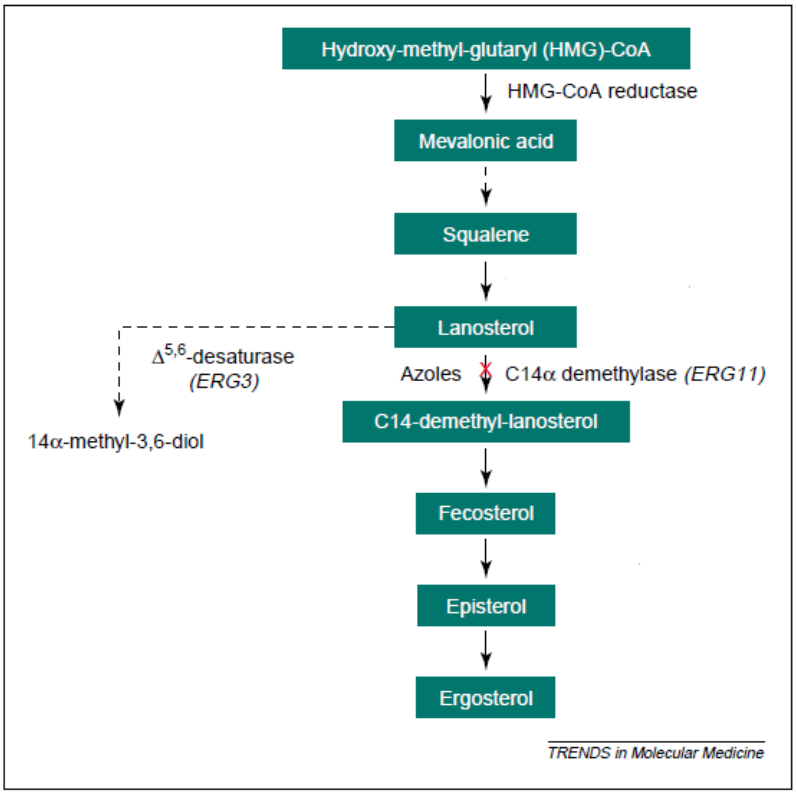

Figure 1.6-Mechanism of action of azoles[III]

1.1.4. Pyrimidines

Pyrimidines are aromatic heterocycles containing two nitrogen atoms within a six-membered ring (Figure 1.7), well-known components of DNA and RNA and structural units of nucleobases, such as cytosine, thymine and uracil.

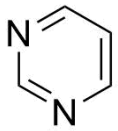

Figure 1.7-General structure of a pyrimidine

5-fluorocytosine (5-FC) was first synthesized as a potential anti-tumor agent in 1957[22]. Later it proved to be active against candidiasis and cryptococcosis in mice, being utilized in such way to treat humans since 1960s[22].

By itself 5-FC is inactive, but when inside a cell, it is deaminated to form 5-fluorouracil (5-FU) by the enzyme cytosine deaminase. For 5-fluorouracil two mechanisms of action have been suggested, one involving a conversion of 5-FU in 5-fluorouridine triphosphate (FUTP) and other involving the conversion of 5-FU into 5-fluorodeoxyuridine monophosphate (FdUMP). For the first, FUTP is incorporated into the fungal RNA replacing the uridylic acid, promoting

[III] Adapted from Lupetti, A. *et al. (reference 21)*

the inhibition of protein synthesis. In the second proposed mechanism, FdUMP inhibits the synthase of thymidylate, an important enzyme in the biosynthesis of DNA[22] (Figure 1.8).

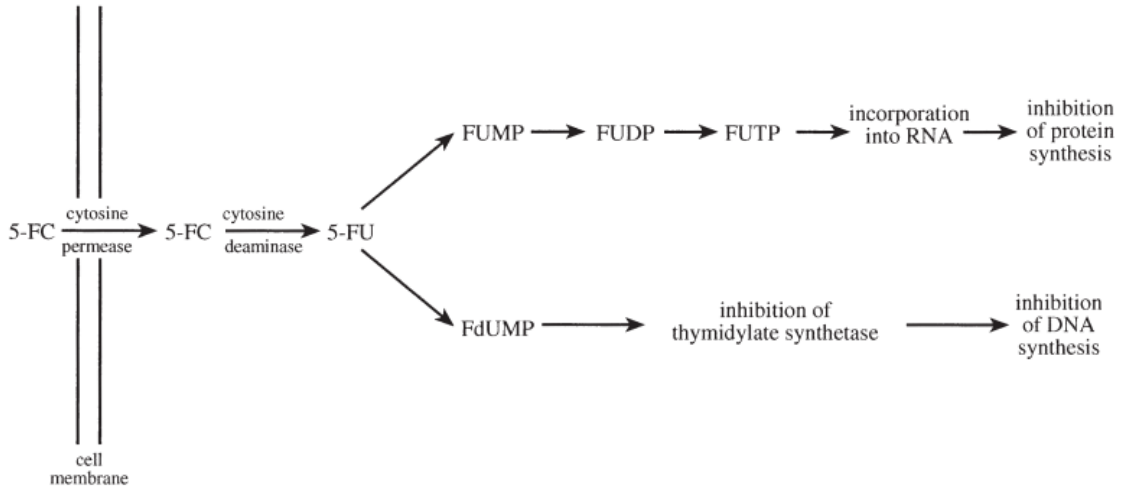

Figure 1.8-Mechanism of action 5-fluorocytosine[IV]

Due to the prevalence of intrinsically resistant strains and the frequent development of resistance during treatment, the 5-FC antifungal activity has used combination with other antifungal drugs, such as polyenes and azoles. This approach leads to an increase of the effectiveness of these drugs (synergetic effect), primarily against *Cryptococcus* and *Candida* infections[15,23].

1.2. Mechanisms of Resistance

Fungi have acquired a large number of resistances to certain antifungals, during the past decades, (e.g. *Candida krusei* to fluconazole, *Aspergillus terreus* to amphotericin B, *Cryptococcus* spp. to the echinocandins, and *Scedosporium* spp. to all current antifungals)[8]. The development of fungal resistances is due to an excessive utilization of available drugs. Related to this is the rising number of immunocompromised patients requiring antifungal treatment[1] and eventually with the excessive usage of fungicides such as azoles, in agriculture or other activities[8].

As previously mentioned, several resistance mechanisms are known for 5-fluorocytosin, such as pathways that involve a mutation in cytosine permease decreasing the uptake of 5-FC or a mutation in cytosine deaminase and uracil phosphoribosyltransferase, blocking the formation of 5-FU and FUMP, respectively[16,24] (Figure 1.9).

For azoles, their recurrent utilization has stimulated the development of resistance mechanisms in fungal pathogens, most relevantly for *Candida* species, but also for

[IV] Adapted from Vermes, A. *et al. (reference 22)*

Cryptococcus species[25]. Several molecular mechanisms of azole resistance have been described and are related to the following mechanisms (Figure 1.9).

- **Decreased dug concentration:** The development of active efflux pumps results in decreased drug concentrations at the site of action, this mechanism has been found in *Candida* species. Also, alterations in the plasma membrane composition affect membrane fluidity and asymmetry, disturbing the influx of drug into the cell, leading to a decreased uptake of drug[24].
- **Target site alteration:** It has been demonstrated that mutations in *ERG11*, the gene encoding for the target enzyme lanosterol 14-α demethylase, prevent binding of azoles to the enzymatic site[24].
- **Up-regulation of the target enzyme:** Overexpression of the target enzyme lanosterol 14-α demethylase, was found to be a mechanism of resistance in *C. glabrata* against fluconazole[24].
- **Development of bypass pathways:** Mutation of the *ERG3* gene prevents the formation of 14a-methyl-3,6-diol Without the formation of this toxic sterol azoles have no antifungal effect[24].

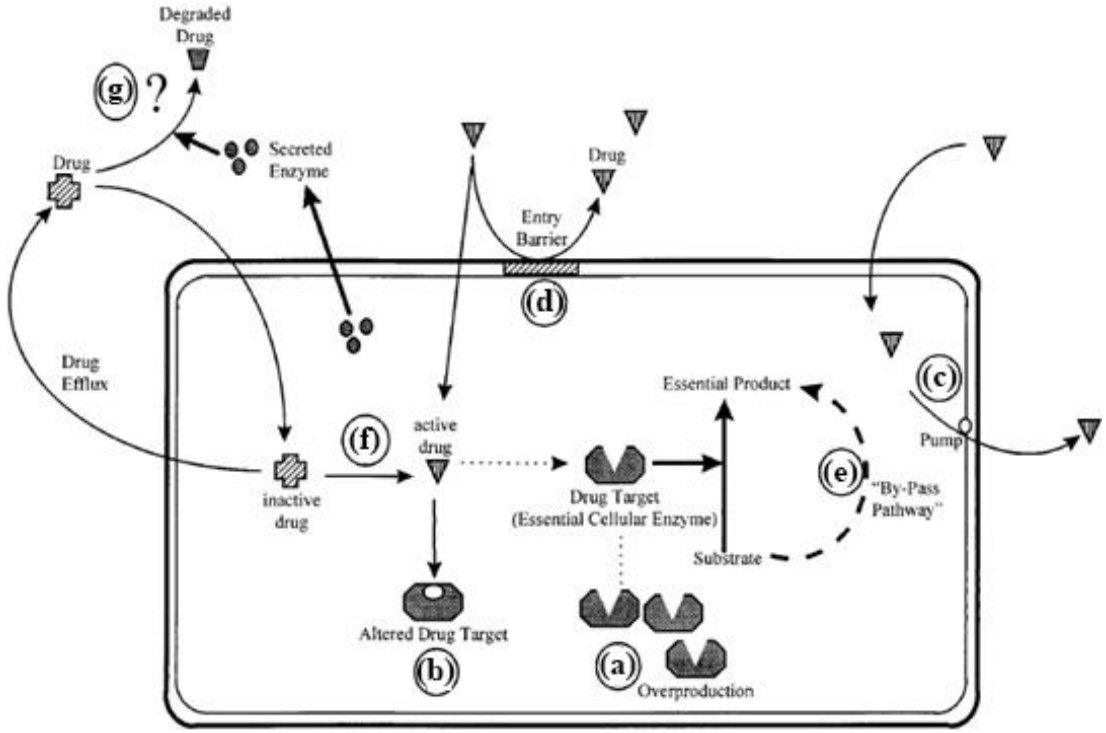

Figure 1.9-Mechanisms of antifungal resistance. (a) Overproduction of the target enzyme, (b) modification of the drug target, (c) increase of drug extrusion, (d) prevention of drug entry, (e) activation of bypass pathways, (f) impaired activation of the drug, (g) secretion of enzymes, which degrade the drug[V].

[V] Adapted from Ghannoum, M. *et al. (reference 15)*

1.3. Synthetic Methodologies utilized

1.3.1. Click Chemistry

Huisgen 1,3-dipolar cycloadditions are reactions between a dipolarophile with a 1,3-dipolar compound that leads to the formation of 5-membered (hetero)cycles. For azides and alkynes this process usually generates a mixture of 1,4- and 1,5-disubstituted triazoles[26] (Scheme 1.1). Since the discovery that the utilization of Cu(I) catalysts leads to the formation of 1,4-isomer[26,27] and Ru catalysts produce to the 1.5-isomer[28], the inconvenience with the selectivity for the Huisgen 1,3-dipolar cycloadditions between azides and alkynes was solved. This modification is a clear example of a click chemistry reaction. Click chemistry is a term that is commonly used to describe reactions that are high yielding, wide in scope and generate only byproducts, which can be removed without chromatography (e.g. through crystallization or distillation as purification methods). They are stereospecific (only one product), considered simple to perform (insensitive to oxygen and water), can be conducted in easily removable or benign solvents and the product is generally stable under physiological conditions[29].

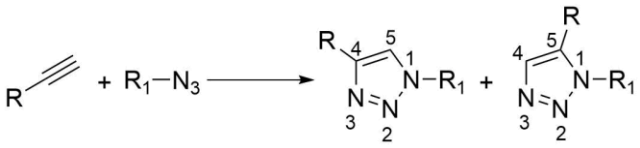

Scheme 1.1- Huisgen 1,3-dipolar cycloadditions

In this project, we employed copper and ruthenium-catalyzed azide-alkyne cycloadditions, to obtain specific structural differences and generate respectively 1,4-disubtituted triazoles and 1,5-disubtituted triazoles.

1.3.1.1. Copper(I)-catalyzed azide-alkyne cycloaddition (CuAAC)

For a CuAAC reaction the active catalyst is a Cu(I) center, which can be used directly or employing a copper(II) precursor alongside a reducing agent. The product of this reaction is an 1,4-disubstituted 1,2,3-triazole[2] (Scheme 1.2).

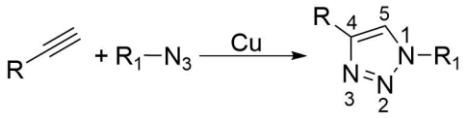

Scheme 1.2- CuAAC reaction for the formation of 1,4-disubstituted 1,2,3-triazoles

Two different reaction mechanisms have been proposed in the literature for the CuAAC reaction. The first mechanism was suggested by Rostovtsev *et al.* in 2002[30] and is represented in Scheme 1.3. In this proposal, the formation of copper(I) acetylide (formation of a σ-bond) is followed by azide coordination to the metal (formation of a π -bond), forming the catalytically

active complex, which converts into a metallacycle with formation of a C–N bond. The next step is the copper oxidation, followed by a ring contraction that leads to the formation of the 5-member ring (triazolide). Finally, copper(I) triazolide is protonated via the acidic alkyne proton and copper is released, completing the catalytic cycle[2,30].

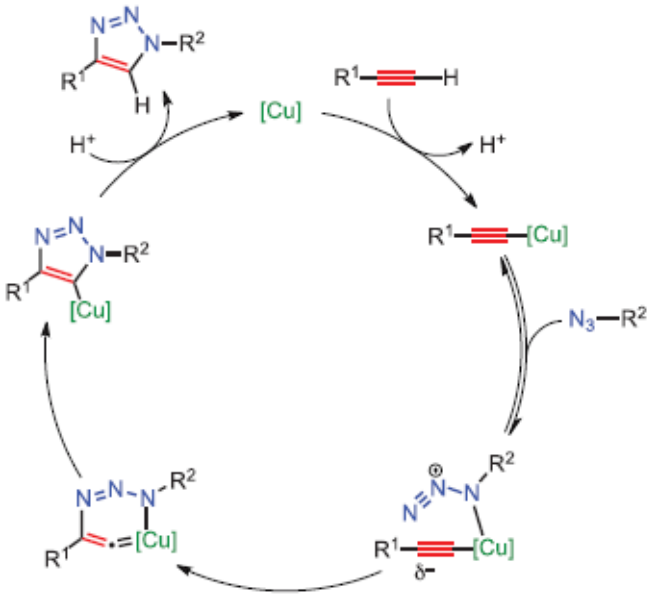

Scheme 1.3- CuAAC possible mechanism involving one copper(I) center[VI]

The second proposed mechanism, which is represented below, proposes an additional copper(I) participation (Scheme 1.4). In this proposal, the formation of a σ-bond and one π -bond between the alkyne and the two copper takes place, followed by the coordination of an azide, creating an azide/alkyne/copper(I) complex. In this step, to form the first covalent C-N bond, a nucleophilic attack by the carbon of the acetylide must occur at the N-3 of the azide. The second C-N bond closes the ring forming a triazolide. Finally, copper(I) triazolide is protonated, via the acidic alkyne proton and cooper is released, completing the catalytic cycle[2,30].

[VI] Adapted from Worrell, B. T. *et al. (reference 30)*

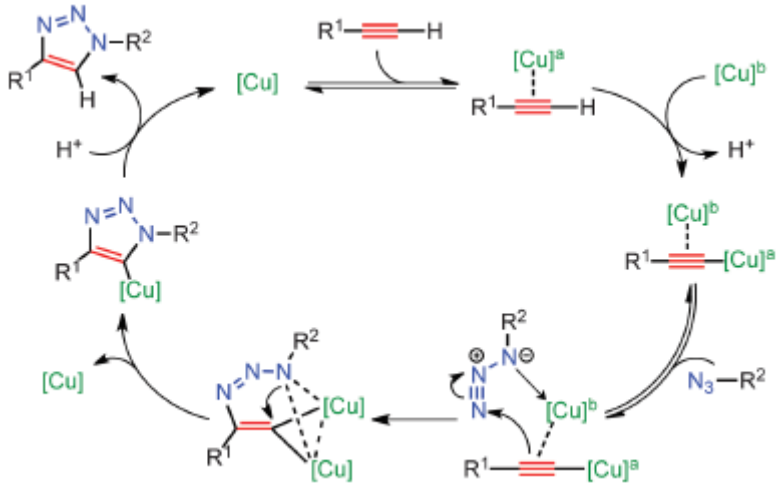

Scheme 1.4-CuAAC possible mechanism involving two copper(I) centers[VII]

1.3.1.2. Ruthenium-catalyzed azide-alkyne cycloaddition (RuAAC)

The product of the RuAAC reaction is an 1,5-disubstituted 1,2,3-triazole. Scheme 1.5 shows a simplified scheme of this reaction. The ruthenium complexes generally utilized in RuAAC reactions are a Cp* complex, found to be especially active and selective catalysts for 1,5-disubstituted triazoles[28].

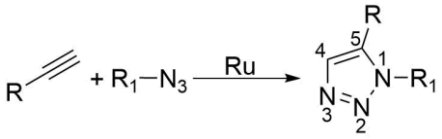

Scheme 1.5- RuAAC reaction for the formation of 1,5-disubstituted 1,2,3-triazoles

The cycle is initiated with the concerted coordination of the alkyne, azide and the ruthenium, forming a ruthenium complex, followed by the oxidative coupling of the alkyne and the azide originating a ruthenacycle. The first C-N bond will be formed between the terminal nitrogen of the azide and the carbon less sterically hindered of the alkyne. Subsequently, the complex undergoes reductive elimination, releasing the aromatic triazole and regenerating the catalyst[3,28]. A representation of this mechanism is depicted in Scheme 1.6.

[VII] Adapted from Worrell, B. T. *et al. (reference 30)*

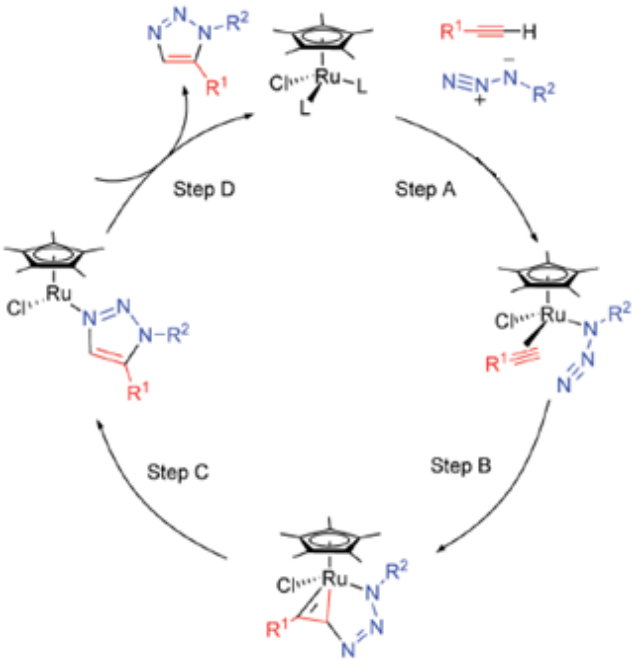

Scheme 1.6- Catalytic Cycle of the RuAAC Reaction[VIII]

1.4. Project Objectives

The main goal of this project was the development of a library of molecules containing a triazole and a pyrimidine within the same core (Figure 1.10), aiming to develop more active antifungal agents based on the well-known synergetic effects for these drugs, when in combination therapies.

Figure 1.10-Model compounds developed in this project

The main building blocks for the development of the novel triazoles were 5-fluorouracil and 3`-azido-3`-deoxythymidine (AZT). Both are pyrimidines that can be further functionalized with different linkers and triazoles. The 5-flurouracil, when combined with the triazole provides as a linker a carbonated chain, and 3`-azido-3`-deoxythymidine a sugar (Figure 1.11).

[VIII] Adapted from Brant C. Boren *et al. (reference 28)*

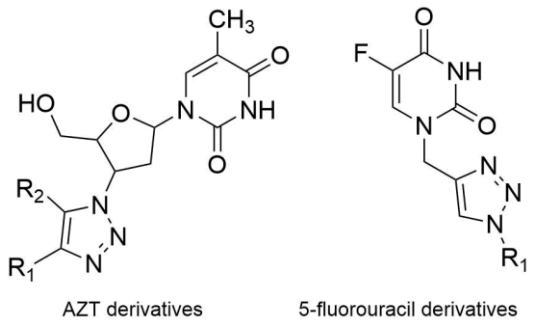

Figure 1.11-Model compounds derivatives of AZT and 5-fluorouracil

The second main objective was the evaluation of the biological activity of the compounds, using as models the fungi *Saccharomyces cerevisiae* and C*andida glabrata*.

In addition, we targeted the development methodologies for the synthesis of fluconazole compounds stabilized by iron, as well as for the synthesis of silver NHC carbenes derived from AZT.

2. Results and Discussion

The main goal of this project was to develop of a library of compounds with high antifungal activity by gathering two commonly used antifungal agents in one single molecule, more specifically azoles and pyrimidines. To achieve this objective, it was performed the synthesis of triazoles derived from 3`-azido-3`-deoxythymidine (AZT) and 5-fluoruracil, employing the Huisgen azide-alkyne cycloaddition with copper and ruthenium catalysts, to achieve the desired connectivity. For the 5-fluoruracil derived triazoles, due to time constraints, only the CuAAC was used.

2.1. Synthesis of 1,4-triazoles derivatives from 3`-azido-3`-deoxythymidine

For our synthesis of 1,4-triazoles, a combination of copper (II) sulfate and sodium ascorbate was utilized. Sodium ascorbate was applied to reduce Cu(II) to Cu(I), since copper(I) is the active catalyst.

To synthesize the 1,4-triazoles derivative from AZT, four different alkynes were chosen. These were phenylacetylene, 2-ethynylpyridine, 1-ethynyl-3,5-difluorobenzene and ethynylanisole, and are represented in Figure 2.1.

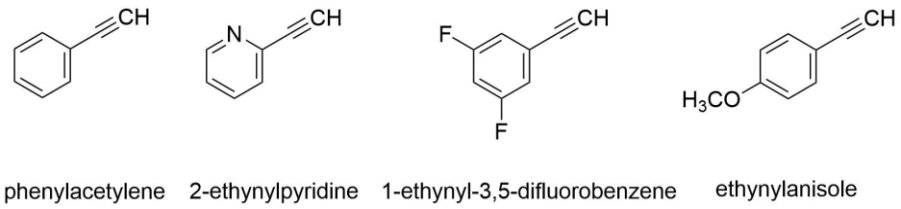

Figure 2.1- Alkyne compounds used for the synthesis of 1,4-disubstiruted 1,2,3-triazoles from AZT

It is assumed that the modus operandi of azole compounds implies the coordination of one nitrogen from the azole ring to the iron of the heme group on the active site of the enzyme lanosterol 14-α demethylase. It has also been suggested that the backbone of the molecule interacts with the active site surroundings (Figure 2.2) and can influence the antifungal activity[31]. In agreement with this, some studies imply that the fluconazole difluorophenyl group induces an hydrophobic interaction with Met153 and the alkyl group of Lys157 in *Cryptococcus neoformans* lanosterol 14-α demethylase[32], that fosters the antifungal activity of the compound. Thus, the above alkyne groups were selected to understand how the different features of the aromatic ring, in addition to the triazole core, would influence its antifungal activity and affect the fitting of the molecule to the catalytic pocket of the enzyme.

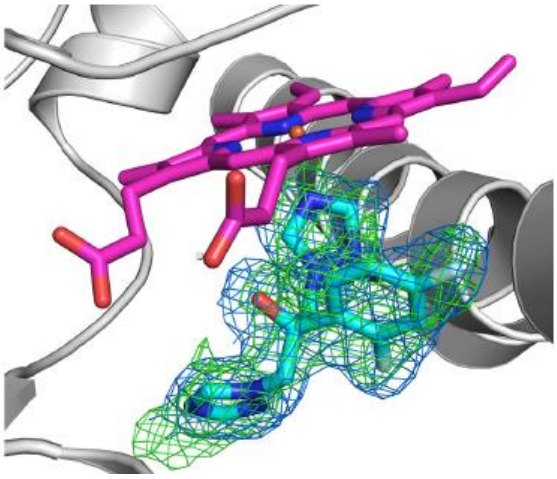

Figure 2.2-Fluconazole binding in the active site of *Saccharomyces cerevisiae* lanosterol 14-α demethylase. The Main chain is represented in gray, and fluconazole is represented in sticks (C atoms in cyan, N atoms blue, O atoms in red, and F atoms in pale blue). The heme is represented in sticks, with C atoms colored magenta[IX].

In line with this, we chose a set of aromatic groups with different substituents, also, to be able to access different properties within the molecule. The substituents in the phenyl group were chosen to either increase polarity to the molecule (2-ethynylpyridine), therefore fostering the solubility of the molecule in water, or introduce variations in the basicity of the triazole (Ethynylanisole). In addition, one of the compounds used, bearing a 3,5-difluorophenyl group, provides access for a direct comparison with fluconazole. Our synthetic methodologies were initiated with phenyl acetylene, for which a synthetic procedure was already described. These methodologies were then extended to the remaining substrates.

The synthesis of compound **1**, the phenylacetylene derivative, was performed according to Zhou *et al.*[33]. Phenylacetylene, 3'-azido-3'-deoxythymidine, $CuSO_4$ and sodium ascorbate were mixed with H_2O/tert-butanol and stirred at 100 ºC for 24 hours. At the end of the reaction, a yellow solid was formed. After filtration, this solid compound was initially extracted with dichloromethane, and the extract was washed with 10% ammonia, then water and brine. This purification, usually employed to ensure removal of Cu salts, did not work as expected, since the product did not dissolve completely in dichloromethane. Then, the remaining solid material was purified by silica gel chromatography ($CHCl_3$: MeOH 10:1 v/v) and obtained as a white powder with a yield of 73%. Compound **1** was again synthesized, after the optimization of the reaction conditions and work-up, to obtain **1** as a white powder with 83% yield.

With these first results, we determined the optimized reaction conditions for the synthesis of the novel AZT derived triazoles (Scheme 2.1). Thus, the syntheses of compounds **2, 3** and **4** were performed in ter-butanol, with $CuSO_4$ and sodium ascorbate at 100ºC for 2 hours.

[IX] Adapted from Sagatova, A. *et al. (reference 31)*

The purification of the compounds was performed using silica gel chromatography ($CHCl_3$: MeOH 10:1 v/v). While compound **2** was obtained as a brown solid with a yield of 50%, compounds **3** and **4** were obtained as white powders with yields of 95% and 33.3% respectively.

Yields varied considerably depending on the alkyne substituent. Thus, for phenyl (**1**) and 3,5 difluorophenyl (**3**) yields were above 80%, with the pyridyl (**2**) performing somewhat lower and the methoxy group (**4**) with a very modest yield.

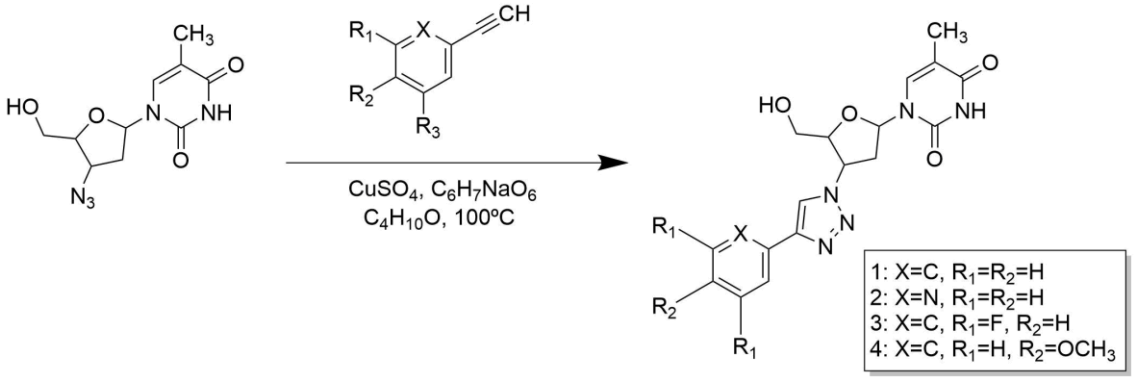

Scheme 2.1-Scheme of the 1,4-disubstituted 1,2,3-triazoles synthesis

According to Kolb *et al.*[29] the compounds obtained from click reactions should be purified utilizing nonchromatographic techniques. However, in our case, all the compounds obtained through click reactions were purified by silica gel chromatography. It was the more effective methodology for the removal of copper salts.

To confirm the structure of the compounds, NMR spectroscopy measurements (^1H and ^{13}C) were performed. The formation of the triazole ring was confirmed through the appearance of a new signal, a singlet for all the 1,4-disubstituted compounds, corresponding to the proton of the C5 position of the newly formed triazole ring. This singlet resonates at around 8.94-8.67 ppm, and is concomitant with the disappearance of the signal corresponding to the terminal alkyne proton (Figure 2.3).

As a common feature, the thymine signals from the C<u>H</u>$_3$ group resonate as a singlet at 1.83 ppm. The N<u>H</u> group, also a singlet, at 11.38-11.37 ppm, while the C<u>H</u> proton of the thymidine can be found between 7.85-7.84 ppm. As for the sugar ring, it gives rise to a set of six signals, between 6.46-2.67 ppm. For instance, the C<u>H</u> group, a quartet, resonates between 4.30-4.28 ppm, the triplet signal of the O<u>H</u> group appeared between 5.31-5.28 ppm and quartet of the C<u>H</u>-N_{trz} group was located around 5.42-5.39 ppm.

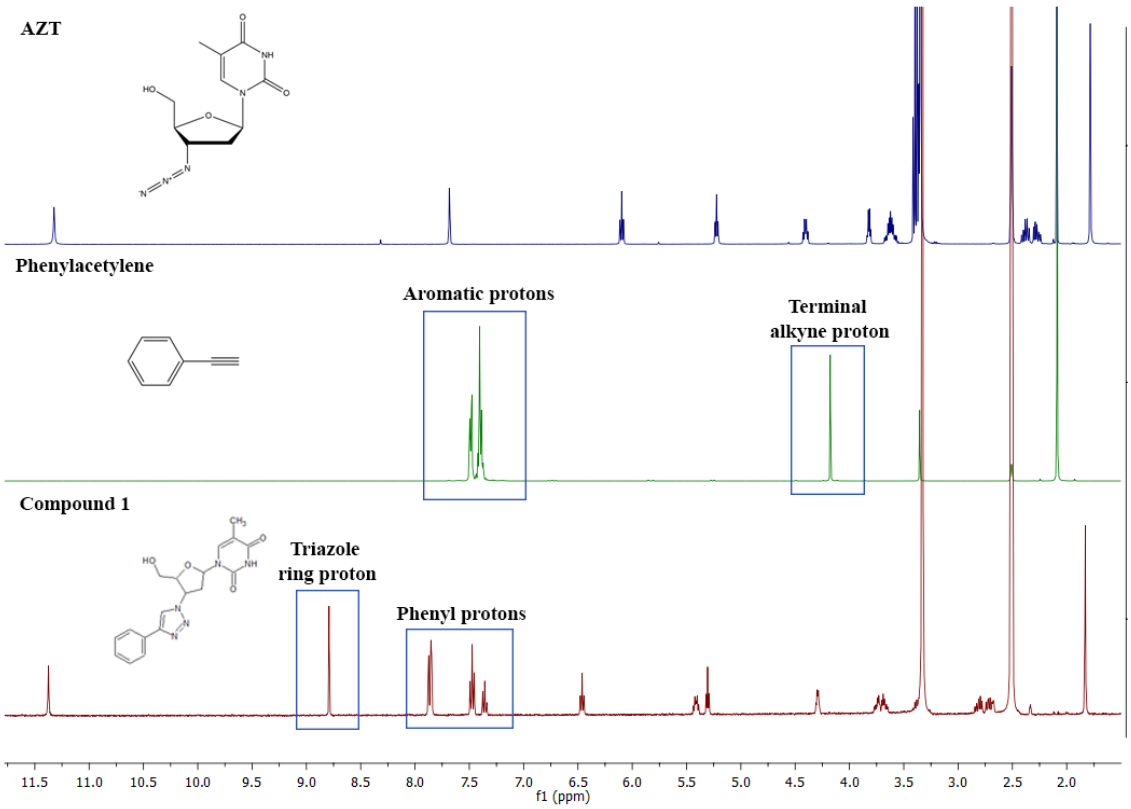

Figure 2.3-^{1}H NMR spectrum of AZT (top) vs phenylacetylene (middle) vs compound **1** (bottom)

In the ^{13}C NMR spectrum, the thymine group signals are similar for all the compounds. For instance, the $\underline{C}H_3$ group resonates at 12.7 ppm, while the $\underline{C}$=O groups can be found at 150.9 ppm and 164.2 ppm. As for the sugar ring carbons, the five signals can be found between 84.4-37.6 ppm. The formation of the triazole ring was confirmed, as was the case for ^{1}H, due to the appearance of the new signals corresponding to C5 and C4 of the newly formed triazole ring. Both signals are located for all 1,4-disubstituted compounds around the same spectrum position (123.4-120.4 ppm and 147.9-145.0 ppm, respectively) (Figure 2.4).

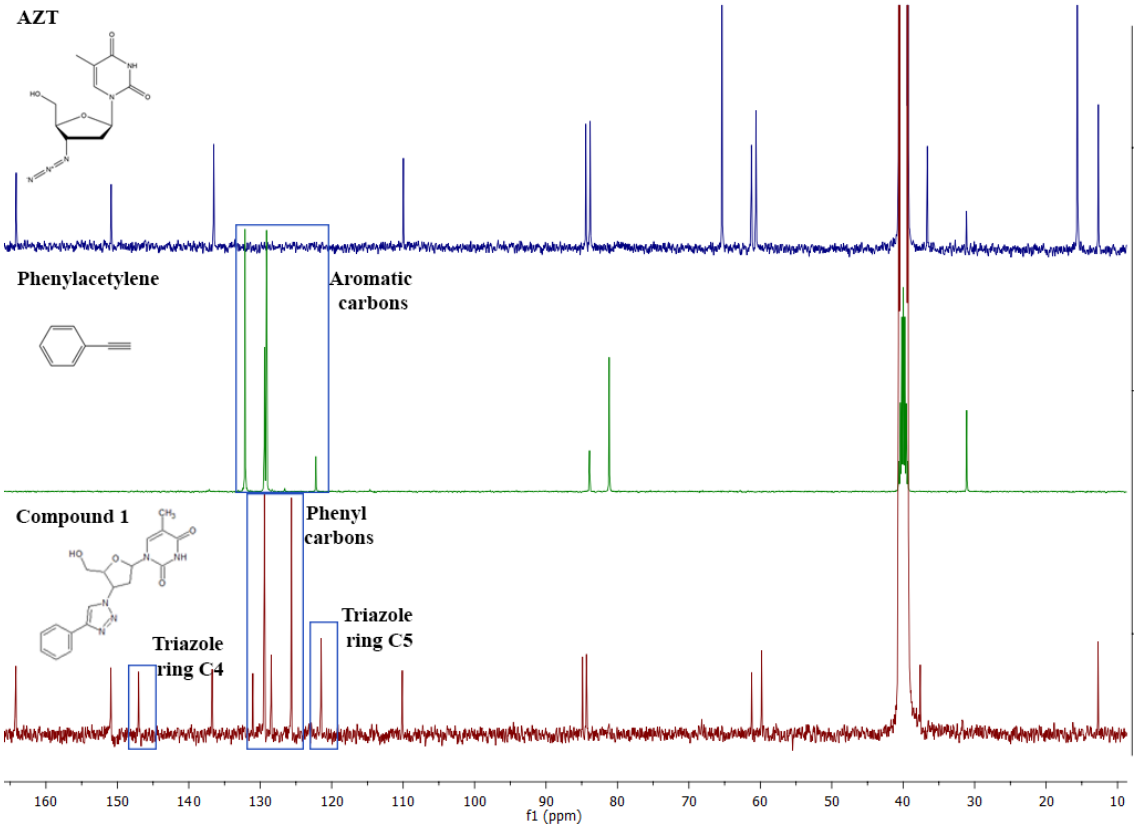

Figure 2.4-^{13}C NMR spectrum of AZT (top) vs phenylacetylene (middle) vs compound **1** (bottom)

2.2. Synthesis of 1,5-triazoles derivatives from 3`-azido-3`-deoxythymidine

Following the synthesis of 1,4-disubstituted triazoles AZT derivatives, the corresponding 1,5-disubstituted isomers were synthesized. Once again, Huisgen azide-alkyne cycloaddition was employed, but this time using a ruthenium catalyst. Ruthenium Cp* complexes are especially active and selective catalysts for 1,5-disubstituted triazoles, normally with excellent yields[28]. The ruthenium catalyst utilized was Cp*RuCl(PPh_3)$_2$, for which a number of procedures are available[28]. Phenylacetylene, 1-ethynyl-3,5-difluorobenzene and ethynylanisole (Figure 2.1) were selected as alkynes. The synthesis of this set of compounds was initiated with phenyl acetylene, for which a synthetic procedure was already described in the literature[3] and this methodology was subsequently adapted to the remaining compounds.

To synthesize compounds **5**, **6** and **7**, AZT was mixed with Cp*RuCl(PPh_3)$_2$ and the correspondent alkyne. The reaction was conducted at 80ºC in dioxane under inert atmosphere for 48 hours (Scheme 2.2). All the new compounds were purified following similar procedures to those used for the 1,4-triazoles. Thus, we employed silica gel chromatography using a mixture of $CHCl_3$: MeOH 10:1 v/v as eluent. Compounds **5** and **7** were obtained as brown powders with yields of 85% and 33% respectively. We were unable to isolate compound **6** under similar conditions and did not explore other possibilities due to time constraints.

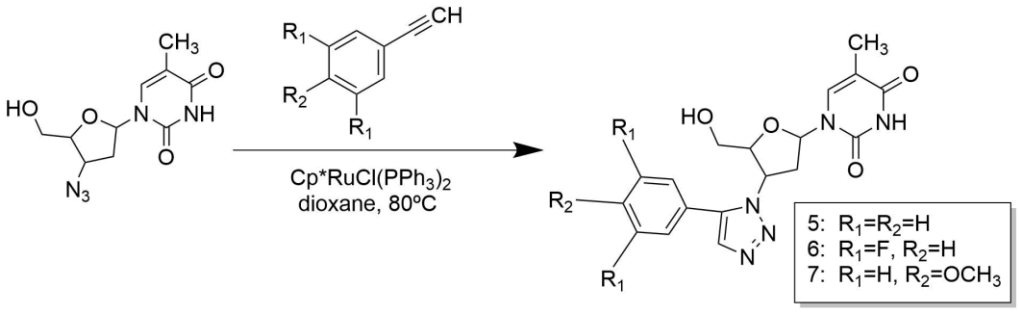

Scheme 2.2-Scheme of the 1,5-disubstituted 1,2,3-triazoles synthesis

To confirm the structure of all compounds, NMR spectroscopy measurements (^{1}H and ^{13}C) were performed. The formation of the triazole ring was confirmed due to the appearance of a new signal, a singlet for all 1,5-disubstituted compounds, corresponding to the proton of the C4 position of the triazole ring at 7.92 ppm in case of compound **5**, 7.85 ppm for compound **7** and the absence of the peak corresponding to the terminal alkyne proton (Figure 2.5).

As a common feature, the thymine signals from the C<u>H</u>$_3$ group resonate as a singlet at 1.79-1.78 ppm. The N<u>H</u> group, a broad singlet resonates at 11.36 ppm while the CH proton of the thymidine can be found at 7.79-7.78 ppm. The sugar ring protons appear as a set of six signals, between 6.57-2.57 ppm. For instance, the C<u>H</u> group, a quartet, is located at 4.40-4.38 ppm and the C<u>H</u>-N$_{trz}$, a multiplet, around 5.19-5.14 ppm.

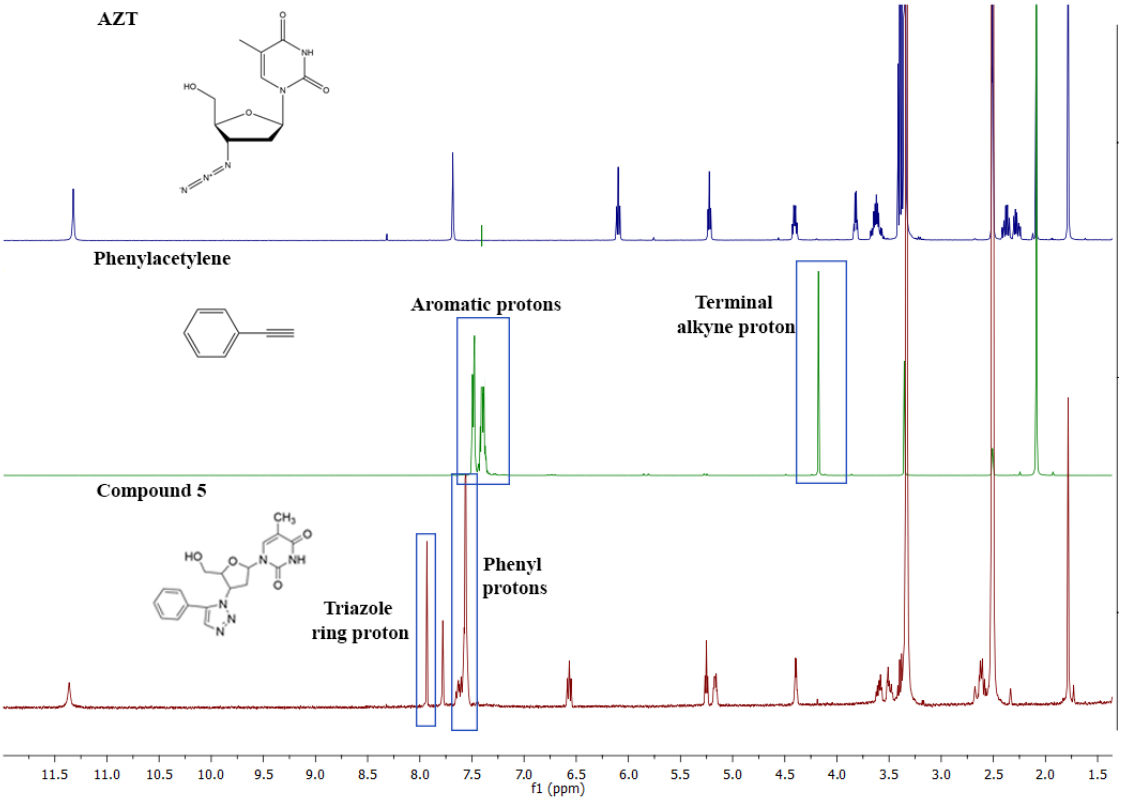

Figure 2.5-^{1}H NMR spectrum of AZT (top) vs phenylacetylene (middle) vs compound **5** (bottom)

In the ^{13}C NMR spectrum, the thymine group signals are similar for all compounds. The $\underline{C}H_3$ group resonates at 12.7 ppm, while the $\underline{C}$=O groups can be found at 150.9 ppm and 164.1 ppm. As for the sugar, the carbon groups can be found between 85.3-38.1 ppm. The formation of the triazole ring was further confirmed through the observation of new signals corresponding to the carbons of the C5 and C4 position of the triazole ring, emerging for all the 1,5-disubstituted compounds around the same spectrum position (138.3-138.1 ppm and 133.3-133.1 ppm, respectively) (Figure 2.6).

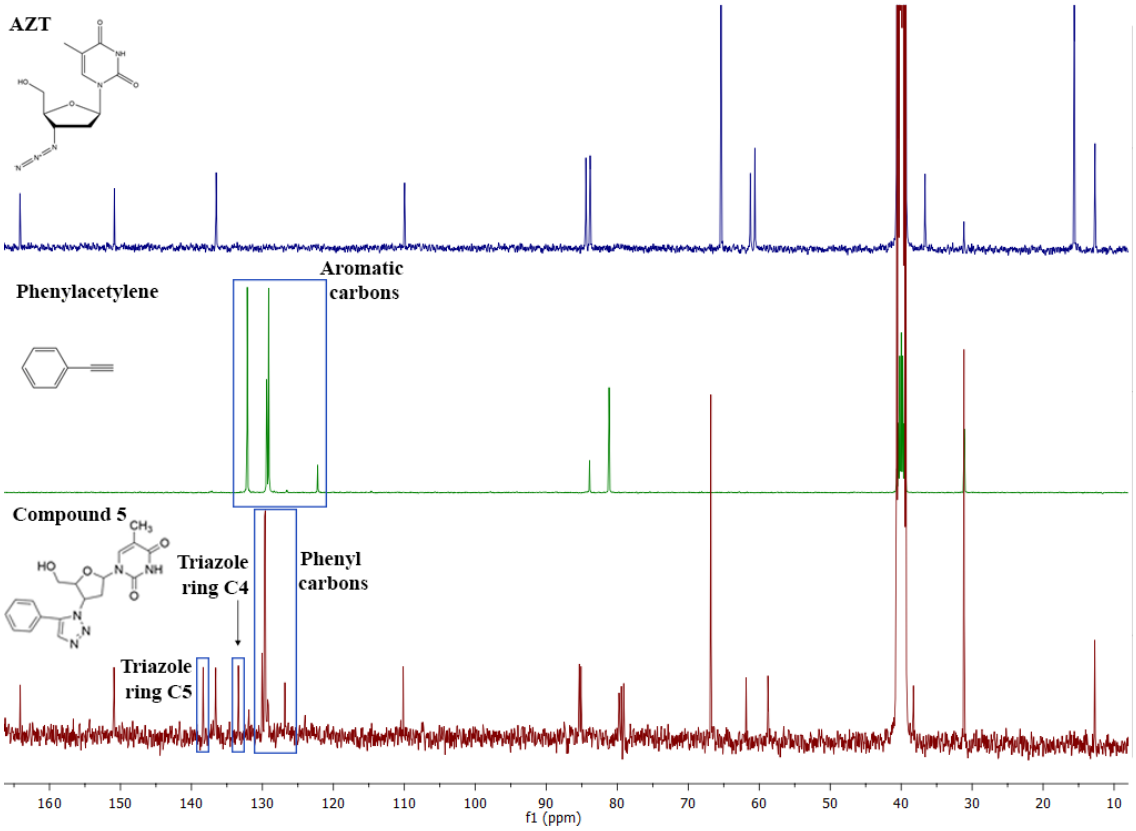

Figure 2.6-^{13}C NMR spectrum of AZT (top) vs phenylacetylene (middle) vs compound **5** (bottom)

Compound **5** was obtained as a brown powder with a yield of 85.55%, similarly to the corresponding 1,4-isomer. Following the tendency noted for the 1,4 triazoles, compound **7** was also obtained as brown powder, with a lower yield (33.3%).

Compounds **1** and **5** (1,4- and 1,5-triazoles) presented different spectroscopic features (Figure 2.7). The main difference between the two compounds relates to the singlet of the triazole ring proton. For the 1,4-triazole the singlet can be found around 8.67-8.94 ppm, while for 1,5-triazoles was detected at higher field around 7.85-7-92 ppm.

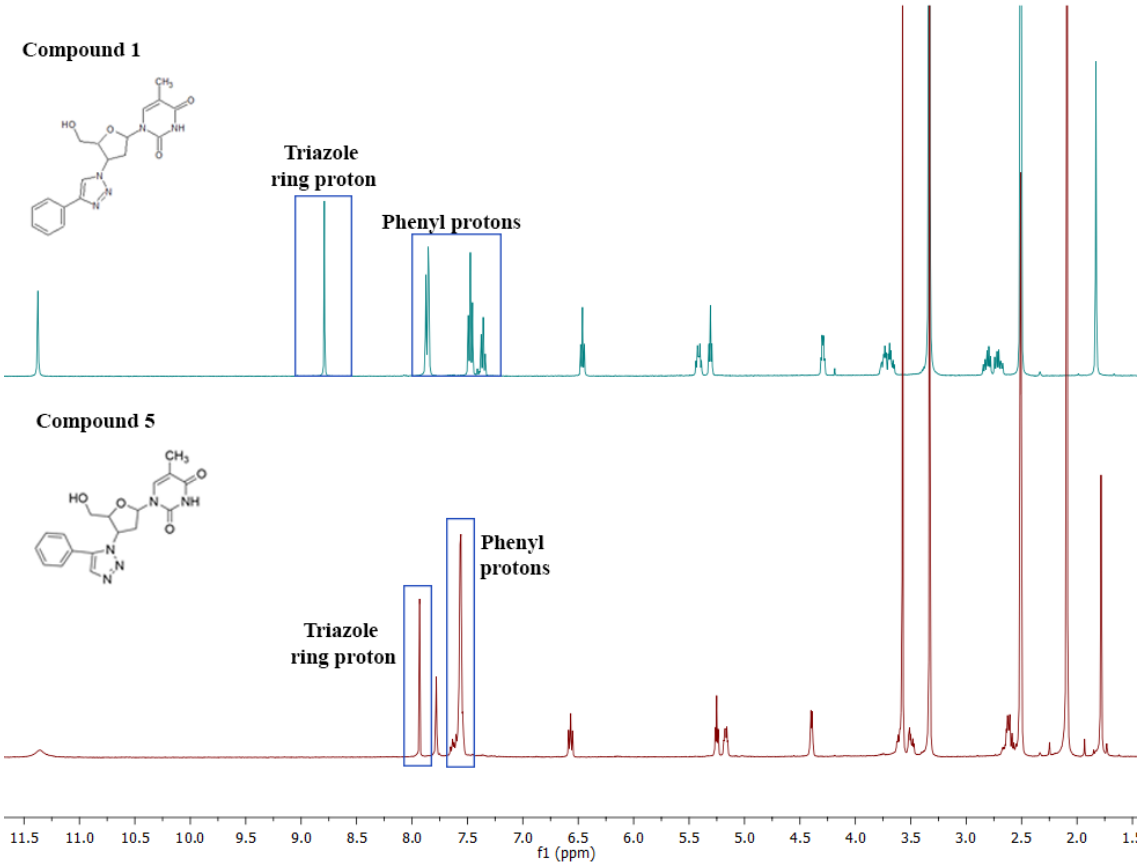

Figure 2.7-^{1}H NMR spectrum compound **1** (top) vs compound **5** (bottom)

In addition, the phenyl protons also presented some differences. For the 1,4-triazole, the aromatic phenyl ring is shown as a doublet, triplet and triplet, in a 2:2:1 ratio, between 7.36-7.90 ppm, while for 1,5-triazoles, a large multiplet combines all the protons, around 7.60-7.53 ppm (Figure 2.7).

2.3. Methylation of 1,4- and 1,5-triazoles derivatives from 3`-azido-3`-deoxythymidine

Following the triazole synthesis, we developed methylation procedures for the triazoles synthesized previously. The main objective regarding compounds methylation was to form a triazolium salt and increase solubility. In addition, the methylation of the triazole ring can eventually influence the coordination to the iron on the active site of the enzyme lanosterol 14α-demethylase and affect the antifungal activity for these compounds.

The methylations were performed by reacting the triazoles with iodomethane or with methyl trifluoromethanesulfonate. Following several experiments, the optimized conditions were determined and are as follow: 1 eq. of the triazole for 10 eq. of the methyl compound. The reaction was heated at 100ºC in DMF for 24 hours. The reaction mixture of compound **8** had a yellow color upon completion and brown color for compound **10**. After cooling to room

temperature, the compounds were precipitated by adding ether to the reaction mixture, followed by a filtration of the solid precipitate.

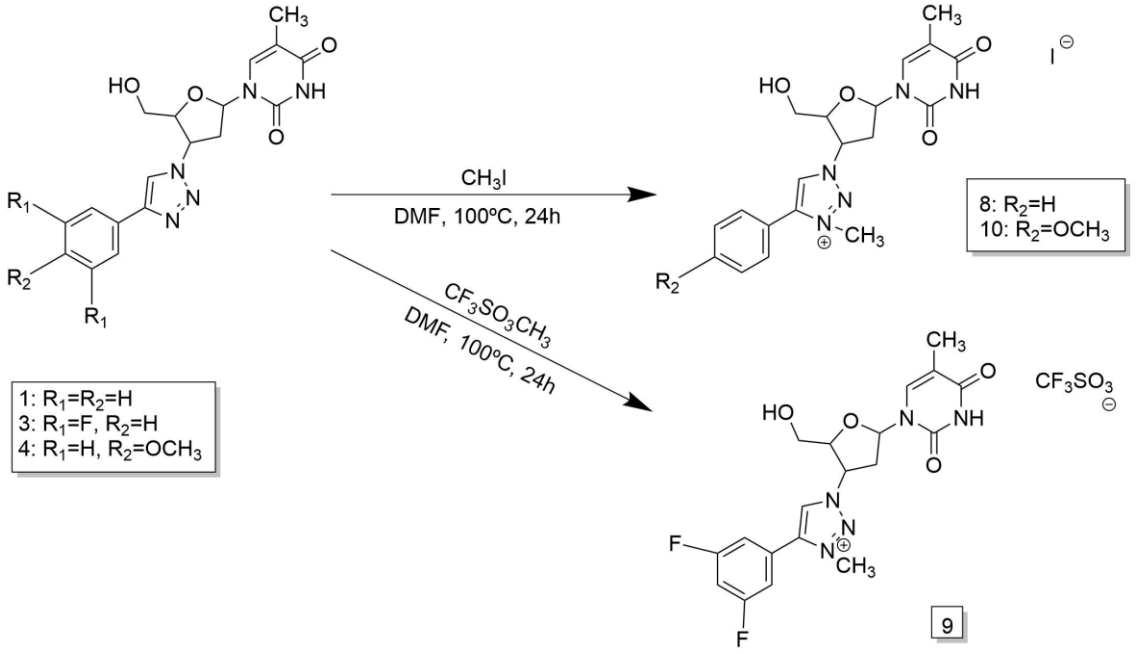

Scheme 2.3-Methylation of the 1,4-disubstituted 1,2,3-triazoles

To obtain compound **9**, methylation with methyl trifluoromethanesulfonate was required, since the reaction with iodomethane was unsuccessful. Compound **9** precipitated as a brown liquid, and after several washes with ether, it was possible to isolate compound **9** as a brown solid with a yield of 8%. The low yield is due in part to the hydroscopic nature of the salt, requiring an extended work-up procedure (Scheme 2.3).

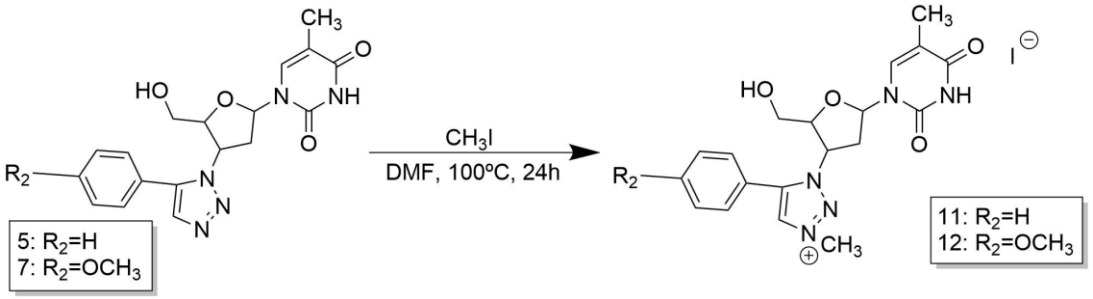

Scheme 2.4-Methylation of the 1,5-disubstituted 1,2,3-triazoles

Compound **8** was obtained as a yellow solid with a 72% yield and compound **10** as a brown solid, with a yield of 31.3%. The 1.5-disubstituted compounds **11** and **12** were obtained as brown solids with 88.4% and 77.2% yields respectively. Compound **8** had a slightly low yield compared to the 1,5-isomer compound **11**, while compound **10** had a lower yield compared with compound **12**.

The structure of the compounds was confirmed by ^{1}H and ^{13}C NMR spectroscopy. The obtained spectra were examined and compared with those of the non-methylated compounds. The ^{1}H NMR spectra from all methylated compounds showed an additional signal, corresponding to the new methyl group of the molecule (N-C<u>H</u>$_3$). The new singlet can be detected at between 4.30-4.38 ppm for the 1,4-triazoles and between 4.44-4.42 ppm in the 1,5-triazoles. The thymine protons from the C<u>H</u>$_3$ group was observed as a singlet that resonate at 1.83 ppm in the 1,4-triazoles and at 1.78 ppm for the 1.5-triazoles. The N<u>H</u> group, a broad singlet, is located between 11.42-11.39 ppm in the 1,4 and 15-triazoles. The sugar protons appeared as a series of six signals between 6.45-2.79 ppm. One important feature that led to the confirmation of the structure of the compounds was the significant shift to low field, observed for the singlet from the triazole ring (*e.g.* for **11** about 1.20 ppm). By contrast, the thymine protons did not undergo significant changes. Slight shifts were noted for the sugar protons, for instance, the C<u>H</u>-N$_{trz}$ group shifted around 0.26 ppm to low field and the C<u>H</u> shifted around 0.18 ppm, also to low field. Figure 2.8 represents the comparison between compound **1** and compound **8** ^{1}H NMR spectrums.

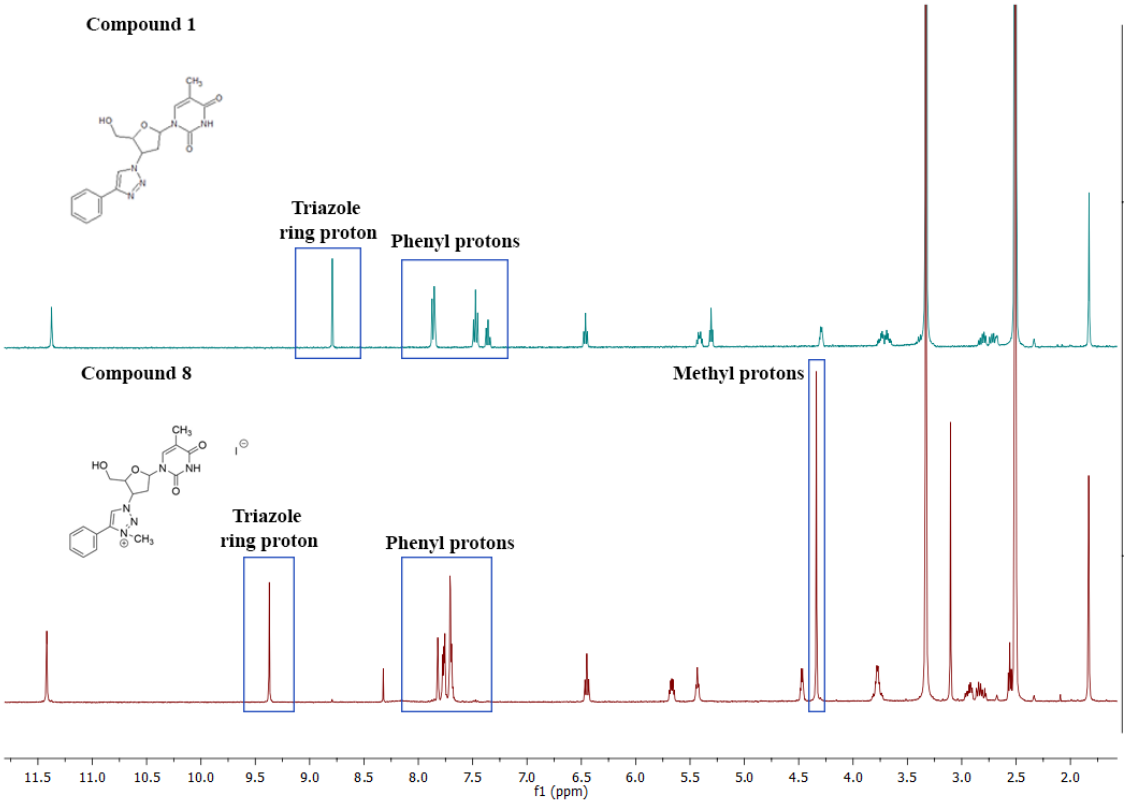

Figure 2.8-^{1}H NMR spectrums of compound **1** (top) vs **8** (bottom)

For the methylated compounds, the ^{13}C NMR spectrum also showed an additional signal, corresponding to the new methyl group of the molecule (N-<u>C</u>H$_3$). The new signal appeared between 39.4-39.2 ppm for the 1,4-disubtituted and between 40.7-40.6 ppm in the 1,5-disubtituted. The pyrimidine <u>C</u>H$_3$ group resonates at 12.7 ppm for, while the <u>C</u>=O groups can be

found at 150.9-150.8 ppm and 164.1 ppm. As for the sugar, the carbon groups can be found between 84.4-37.6 ppm. Figure 2.9 represents the comparison between compound **1** and compound **8** ^{13}C NMR spectrums. The structure of the compounds was confirmed by the rearrangement of the phenyl group signals positions and the shift of the triazole carbon C5 and C4 in the 1,4-triazoles (shifted around 8 ppm and 5 ppm, respectively) and in the 1,5-triazoles (shifted around 5 ppm and 3 ppm, respectively).

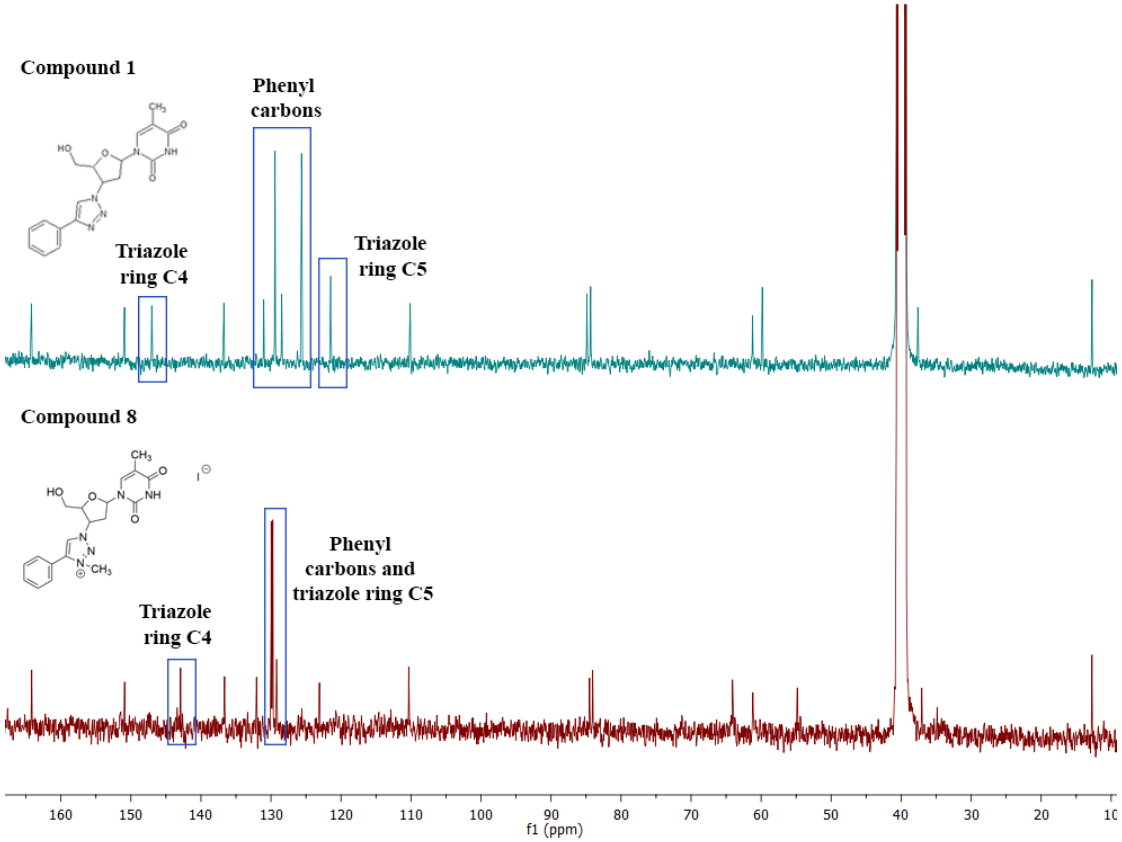

Figure 2.9-^{13}C NMR spectrum of compound **1** (top) vs compound **8** (bottom)

The thymine and carbons do not undergo significant changes, however the sugar carbon from the CH-N- group near the triazole had a shift of 5 ppm in the 1,4-triazoles and 3 ppm in the 1,5-triazoles (Figure 2.9).

2.4. Synthesis of 1,4-triazoles derivatives from 5-Fluorouracil

2.4.1. Alkynylation of 5-Fluorouracil

5-fluorouracil is the active antifungal compound resultant of the deamination of 5-fluorocytosine (Figure 2.10). To synthesize the triazole from 5-fluorouracil, first it is necessary to introduce an alkyne group to form the precursor. In addition, syntheses of azides for the click reaction were also required.

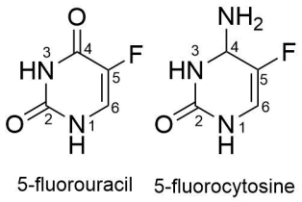

Figure 2.10-5-fluorouracil and 5-fluorocytosine

To synthesize the 1,4-disubstituted triazoles from 5-fluorouracil, we chose to introduce an alkyne group at N1, making use of previously established procedures[34].

In this approach, we adapted the procedure described by Weiss, J. T. *et al.*[34]. In this methodology, protection is not required and the alkyne group is bound directly to N1 in one sole step, employing propargyl bromide as reagent (Scheme 2.5).

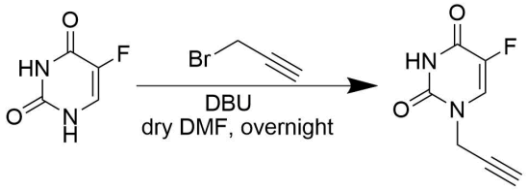

Scheme 2.5- Scheme of the alkynylation of 5-Fluorouracil

This approach worked successfully, but purification via chromatography was required. Compound **13** was obtained as a white powder and the yield obtained was very low (4%).

To overcome this, the reaction was scaled-up from 1.5 mmol (200 mg) of 5-Fluorouracil to 4.6 mmol (600 mg). This resulted on a yield improvement to 13%. This outcome was slightly better, but could not be improved. As such, the repetition of the same reaction several times was required, in order to obtain the required amount of compound **13** to perform the remaining reactions. It must be stated that the published yield for this procedure is 40%.

The formation of compound **13** was confirmed by ^{1}H NMR spectroscopy. In the ^{1}H spectrum, the singlet corresponding to the N<u>H</u> proton can be detected at 11.92 ppm, while the 5-fluorouracil aromatic proton resonates at 8.14 ppm as a doublet. The doublet for the C<u>H</u>$_2$ group resonates at 4.47 ppm and the alkyne terminal proton at 3.46 ppm as a triplet. The results matched the data reported by Weiss, J. T. *et al* [34] further confirming the structure of compound.

2.4.2. Azide Synthesis

With compound **13** already synthesized and to obtain our target molecule, our second step was to synthesize the azide. We synthesized two different azides, both aromatic, but with a varying substituent.

The synthesis of two azides, phenyl azide (**14**) and 4-bromo phenyl azide (**15**), was performed according to the procedure employed by Barral *et al.*[35]. This procedure employs anilines as azide precursors. The synthesis involves the formation of diazonium salts from the corresponding aniline, followed by the formation of the azide. The azide is formed by way of two competing reactions[36] that can be observed in Scheme 2.6.

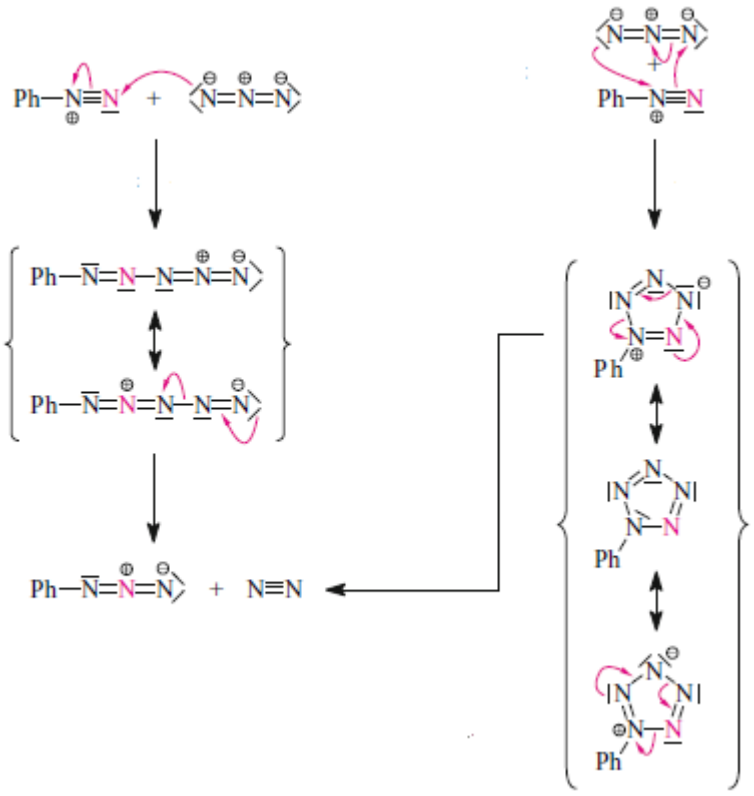

Scheme 2.6- Mechanism of formation of azides by diazonium salts[X]

The residue was purified by silica gel chromatography using ether as eluent. Phenyl azide (**14**) was obtained as a yellow liquid with 76% yield and 4-bromo phenyl azide (**15**) as an orange liquid in 75% yield (Scheme 2.7).

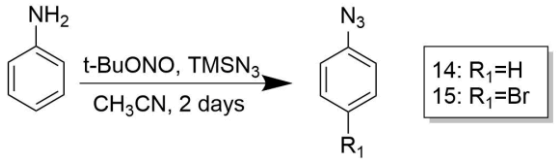

Scheme 2.7- Scheme of the azides synthesis

To confirm the structure of the compounds, NMR measurements were performed. For the new azides, ^{1}H NMR spectrum shows three signals for compound **14** and two signals for compound **15**, these between 7.50-7.00 ppm. Important aspects that led to the confirmation of the compounds structure were the absence of the signal at 4.99 ppm corresponding to the amine

[X] Adapted from Bruckner, R. *(reference 36)*

group (NH_2) and the rearrangement of the aromatic signals that shifted from 7.02-6.47 ppm to 7.50-7.00 ppm (Figure 2.11).

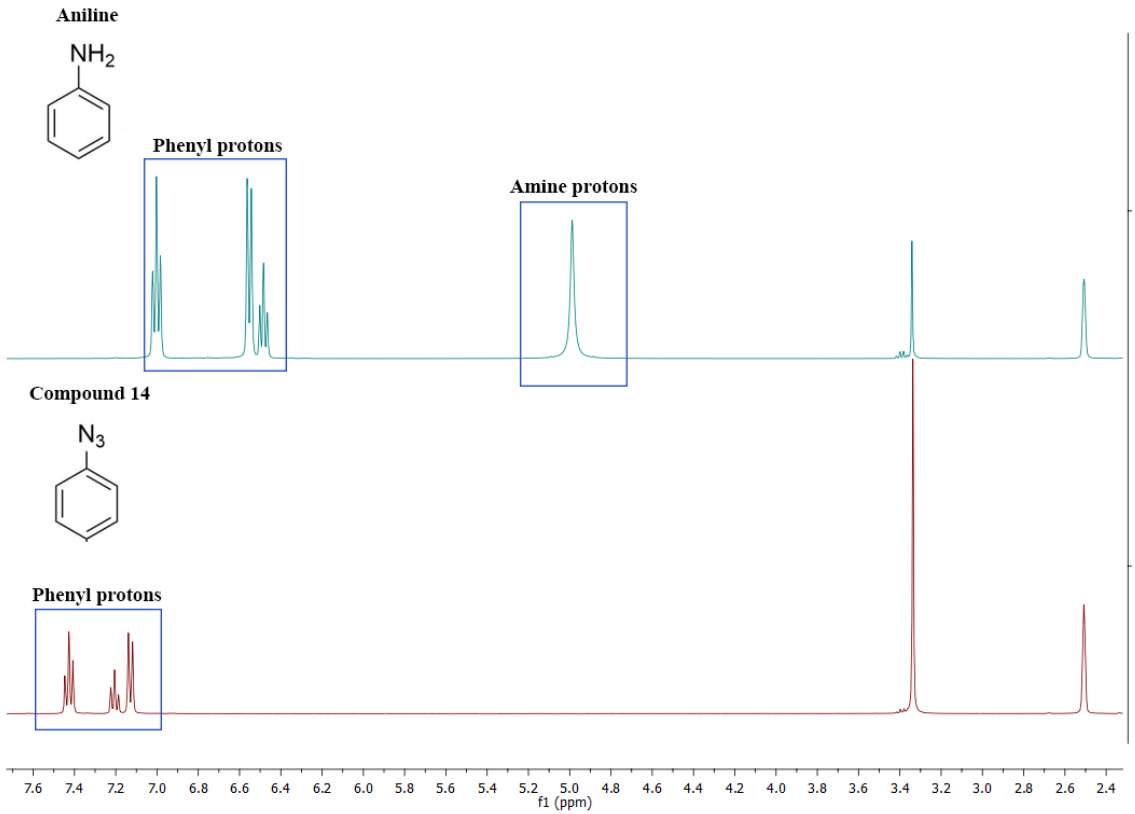

Figure 2.11-^{1}H NMR spectrum of aniline (top) vs phenyl azide (bottom)

2.4.3. Synthesis of 1,4-triazoles derived from 5-fluorouracil and methylation

The 1,4-disubstituted triazoles from 5-fluorouracil were synthesized in similar conditions used for the AZT derivatives described above, using $CuSO_4$ and sodium ascorbate, at 80ºC (Scheme 2.8). Compounds **16** and **17** were obtained as white and light brown powders in relative low yields (36% and 15% respectively).

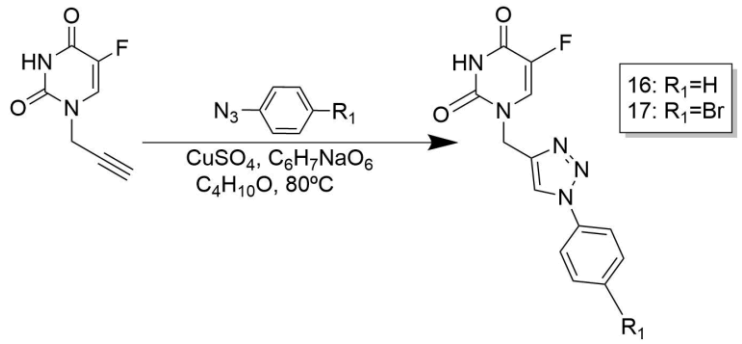

Scheme 2.8-Scheme of the 1,4-disubstituted 1,2,3-triazoles from 5-Fluorouracil synthesis

^{1}H NMR spectroscopy measurements were also obtained, confirming the structure of compounds **16** and **17**. The uracil signals from both compounds were observed as singlets

around 11.89-11.87 ppm for the NH group and at 8.23 ppm for the aromatic proton. The singlet from the CH_2 protons appeared at 5.01 ppm in both cases. As was the case of the AZT derivatives, a new singlet corresponding to the CH group of the new triazole ring, at around 8.81-8.84 ppm, confirms the formation of the triazole (Figure 2.12).

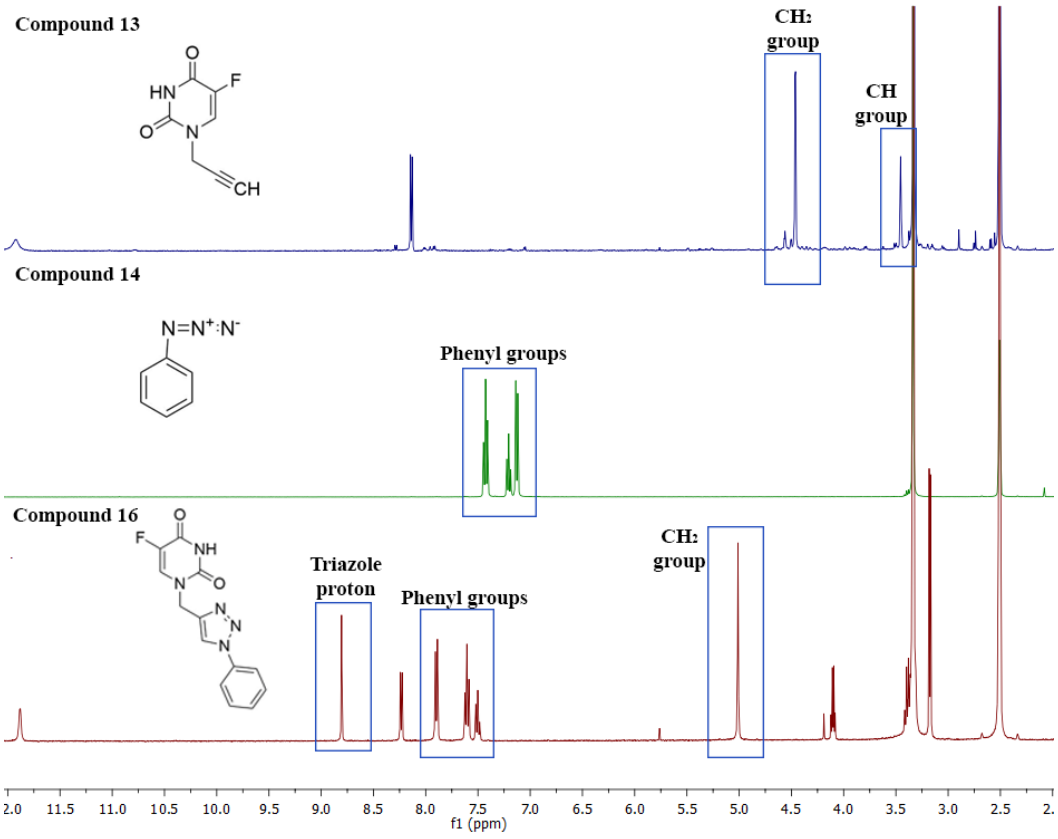

Figure 2.12-^{1}H NMR spectrum of compound **13** (top) vs compound **14** (middle) vs compound **16** (bottom)

In the ^{13}C NMR spectra, for uracil signals, the C=O groups resonate at 158.1-157.9 ppm and 149.9 ppm, while the CH group at 130.5 ppm. The formation of the triazole ring confirmed through the observation of the new signals for C5 and C4 at 122.1 ppm and 144.0 ppm, respectively. Another important feature was the shift of the CH_2 group signal from 37.0 ppm to 43.2 ppm (Figure 2.13).

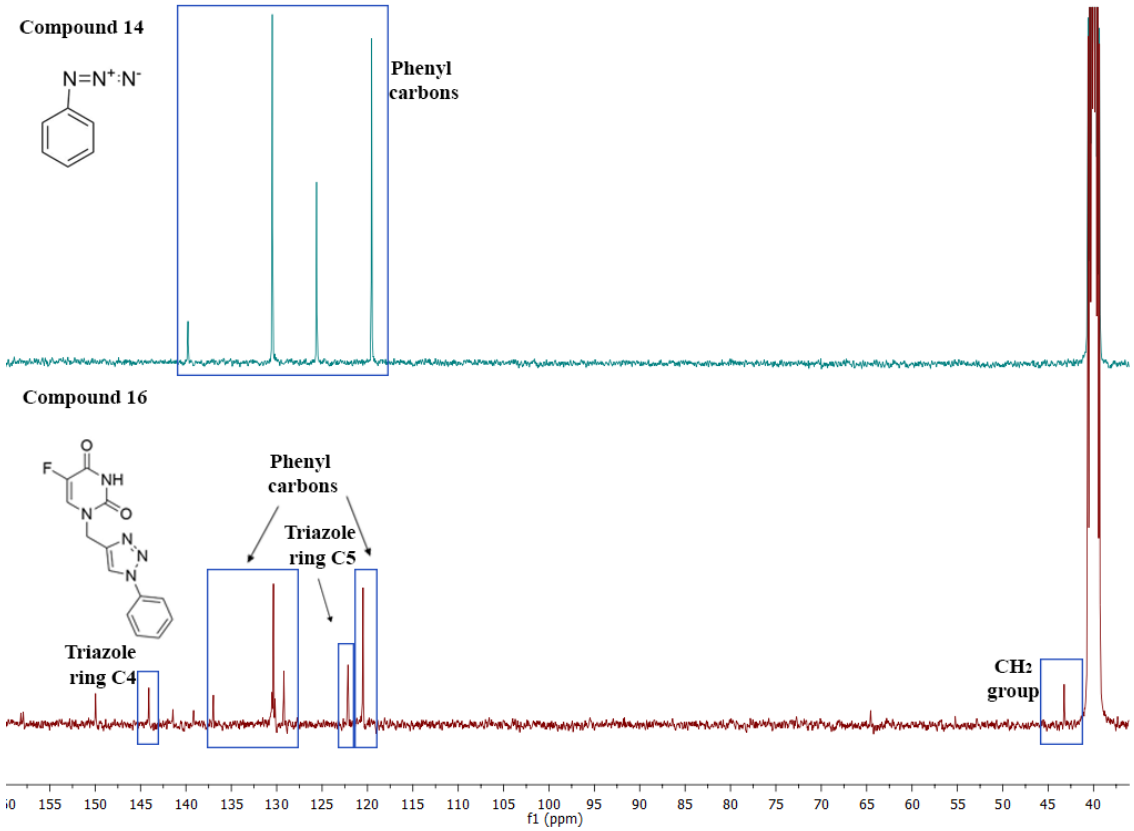

Figure 2.13-^{13}C NMR spectrum of compound **14** (top) vs compound **16** (bottom)

The methylation of compound **16** was performed following similar procedures as those used for the AZT derivatives. Compound **16** was reacted with 3 eq. of iodomethane in DMF, at 100ºC for 24 hours. After cooling to room temperature, the reaction mixture was precipitated with ether, obtaining compound **18** as a yellow powder in moderate yield of 46% (**18**) (Scheme 2.9).

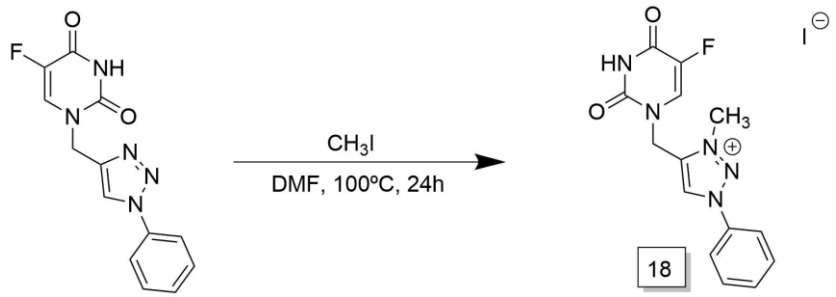

Scheme 2.9- Scheme of the synthesis of compound **18**

The confirmation of the structure of the compound **18** was performed by ^{1}H and ^{13}C NMR spectroscopy. The obtained spectra were evaluated and compared with the spectra of the non-methylated compounds. The ^{1}H spectrums from the methylated compound showed an additional signal, corresponding to the new methyl group of the molecule (N-C$\underline{H}_3$), at 4.46 ppm. The uracil N$\underline{H}$ group, appeared as a broad singlet, at 12.08 ppm and the aromatic proton, as

duplet at 8.19 ppm. In addition, the triazole proton at C5 shifted from 8.81 ppm to 9.63 ppm. The uracil protons did not undergo significant changes, following the tendency observed for the AZT derivatives, Figure 2.14 represents the comparison between compound **16** and compound 1**8** ^{1}H NMR spectrums.

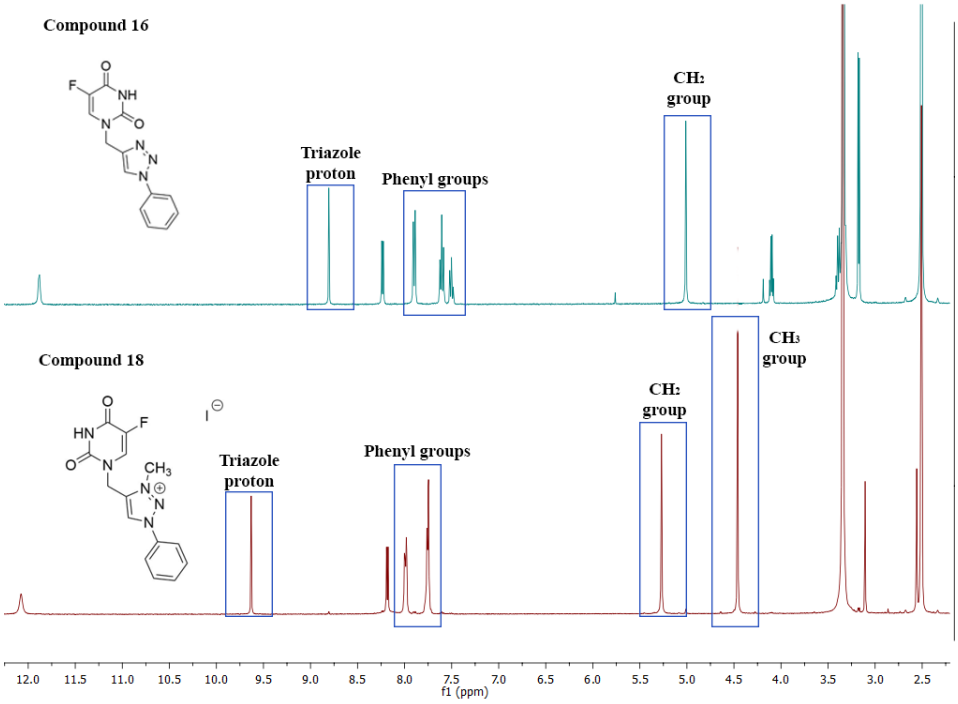

Figure 2.14- ^{1}H NMR spectrum of compound **16** (top) vs compound **18** (bottom)

In the ^{13}C NMR spectra of compound **18**, the uracil signals were present at 158.1 ppm and 150.1 ppm for the C=O groups, while for CH group at 129.6 ppm. Following the tendency observed previously, a new signal at 40.5 ppm, corresponding to the N-CH_3 is observed, as well as a shift at C5 and C4 of the triazole ring, by 6 ppm and 4 ppm respectively. (Figure 2.15).

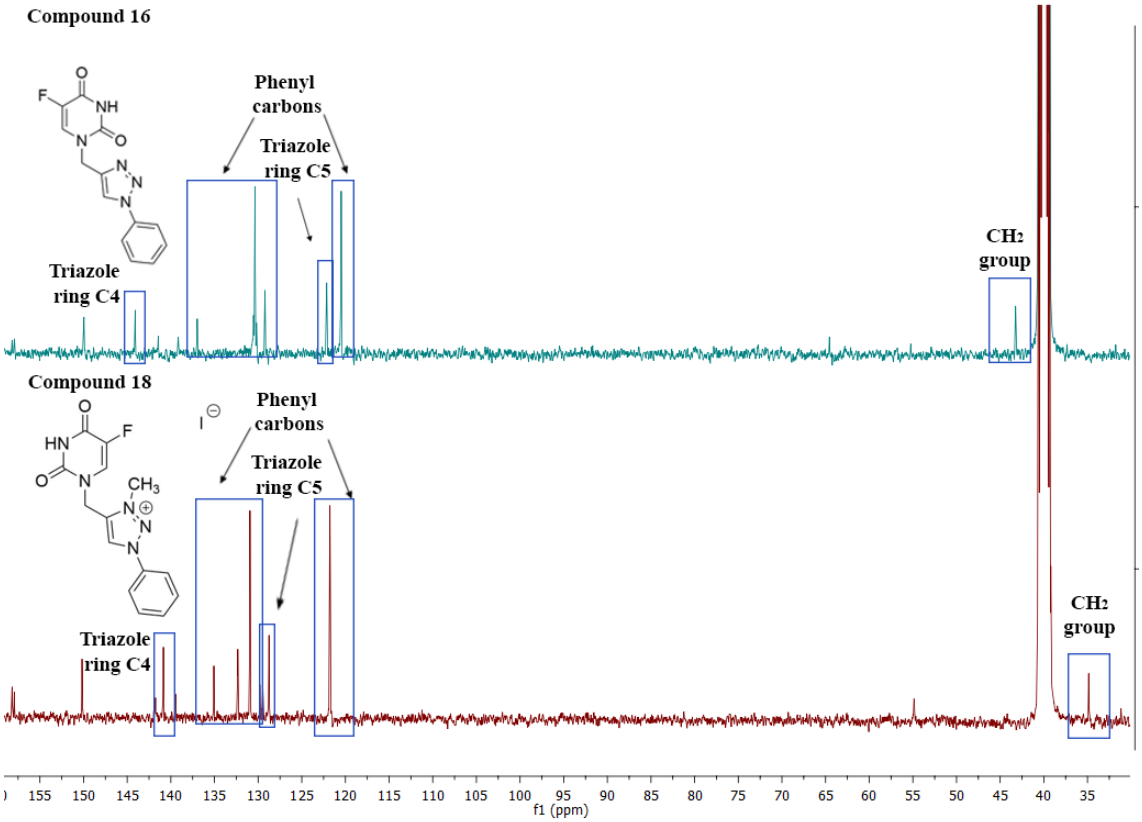

Figure 2.15-^{13}C NMR spectrum of compound **16** (top) vs compound **18** (bottom)

2.5. Synthesis of silver NHC compounds based on AZT

Metallic silver and silver compounds have numerous uses in medicine. Since the early days, silver with its notably antimicrobial activity, is not only utilized in medical devices (e.g. bone prostheses, surgical sutures and dentistry)[37,38], but also particularly used against chronic ulcers, extensive burns, and difficult-to-heal wounds. Silver antimicrobial activity is related with its interference with electron transport system of the cell, interaction with cell membrane and the thiol groups of key enzymes in microorganisms[39]. Some studies report that silver NHC complexes have high antimicrobial activity, and perform better than their NHC precursors, such as imidazoles and triazoles[39,40].

For the metallation of compound **8** we utilized Ag_2O as silver source. The reaction was performed in DMF under inert atmosphere and in the absence of light, due to the sensitivity of silver salts. A variety of reaction conditions were tested, by changing the ratio of compound **8** versus Ag_2O, temperature and reaction time (Scheme 2.10).

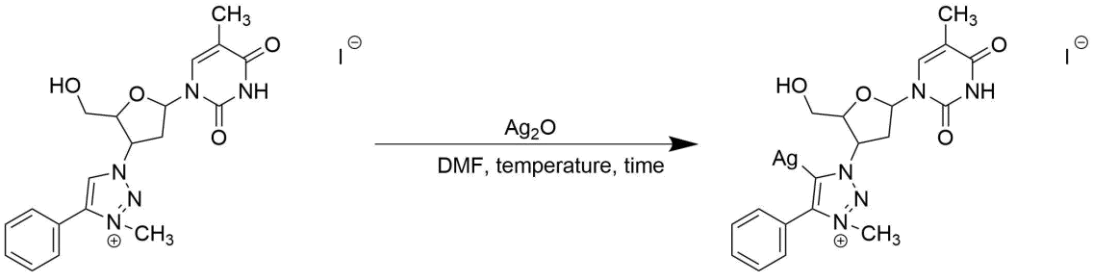

	Ratio compound/Ag_2O (mmol)	Temperature	Time
A	0.1/0.05	r.t	2h
B	0.1/0.05	100ºC	6h
C	0.05/0.03	r.t	26h
D	0.07/0.05	r.t	3d

Scheme 2.10- Silver reactions

Analysis by ^{1}H NMR spectroscopy shows the presence of a new compound, alongside with compound **8**, in a 55:45 % ratio.

The new species is characterized by a signal at 4.21 ppm, corresponding to the protons of the methyl group (N-CH_3) of the triazole ring, shifted by 0.12 ppm with respect to compound **8**. In addition, a new set of signals in the aromatic region corresponding to the phenyl group could be observed (Figure 2.16).

It can be concluded that the metalation can be achieved, but only partially. The formation of the new silver compound is possible, but the conversion of compound **8** to the metallated derivative is not complete, at least under the tested conditions. Of note, independently of the reaction conditions, the result is similar in all cases, leading to 1:1 mixture approximately.

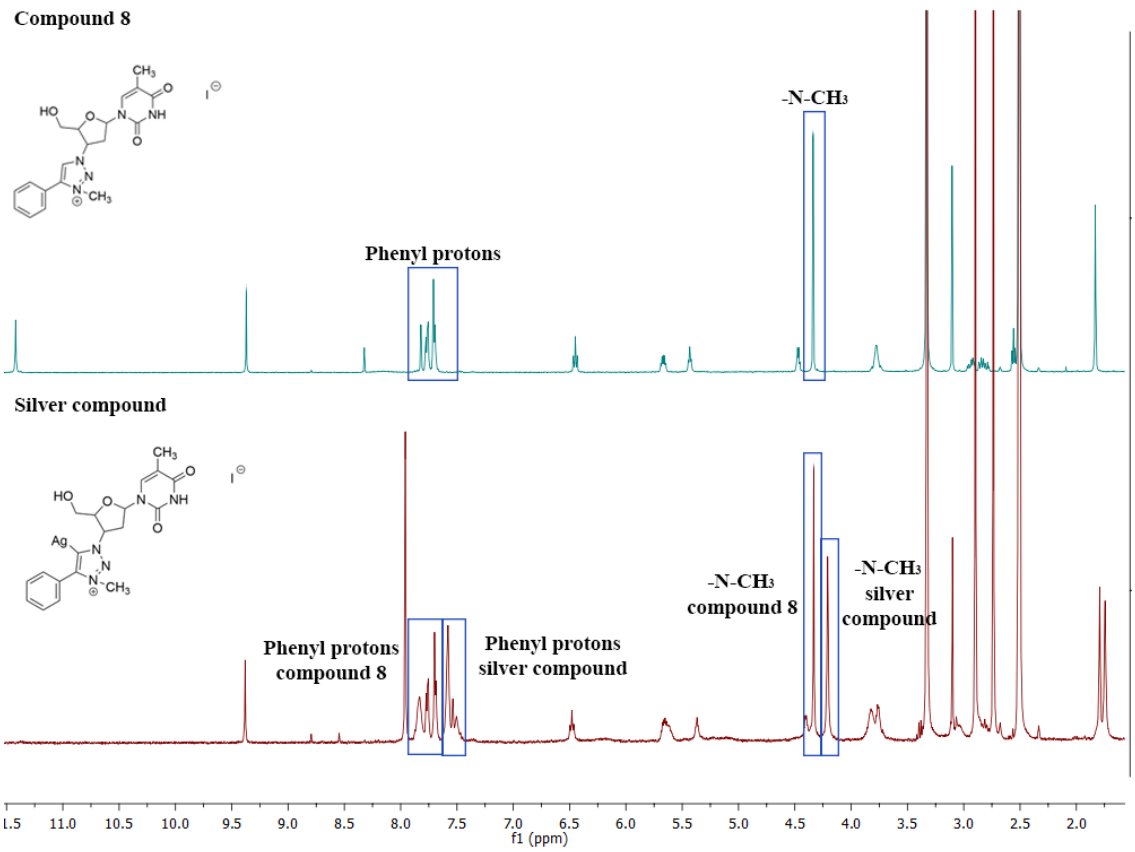

Figure 2.16-^{1}H NMR spectrum of compound **8** (top) vs compound with silver (bottom)

2.6. Synthesis of Iron fluconazole complexes: Studies on coordination and stability

Some studies suggest that iron concentration can have an influence in the antifungal activity of fluconazole[41]. However, records on the coordination and stability of fluconazole and iron coordination compounds are extremely scarce. We decided to study the coordination of fluconazole to iron complexes and the evaluation of the stability of these complexes.

To synthesize these complexes, we tested a variety of conditions, using mainly $FeCl_2$ as iron source. Different solvents were selected, such as DCM/MeOH, MeOH, D_2O. Some reactions were performed under air while others under inert atmosphere.

The first reactions (**a** and **b**) were carried out with $FeCl_2$ in (**a**) a mixture of DCM/MeOH (2/1) and (**b**) exclusively MeOH, and were monitored by ^{1}H NMR for 24 hours. The ^{1}H spectra showed a significant evolution with time. When comparing the two reactions, NMR analysis shows the formation of the same product in both cases, but the rate of its formation seems to be affected by the solvent (Figure 2.17).

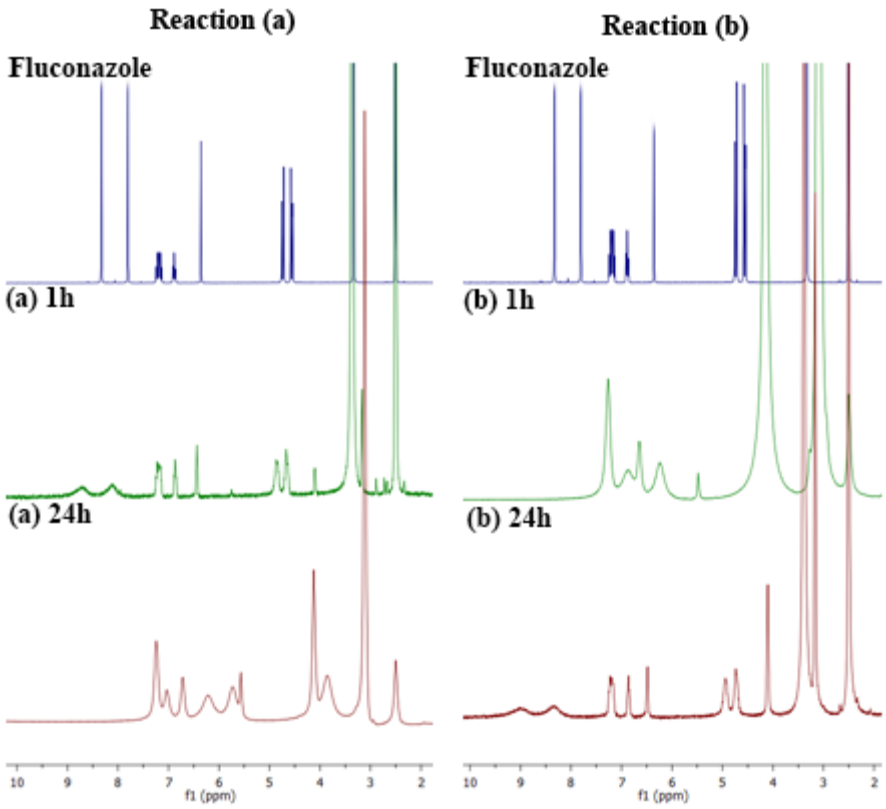

Figure 2.17-^{1}H-NMR spectrums reaction (**a**) vs reaction (**b**)

Reaction (**b**) was repeated, but using (**d**) 2 eq. of $AgNO_3$ for each 1 eq. of $FeCl_2$ under air and (**e**) under inert atmosphere. The utilization of silver salts to promote this reaction was based on the well-known insolubility of the $AgCl_2$ salts, which leads to their precipitation in solution, leaving a vacant coordination site in Fe, thus favoring coordination of fluconazole. However, this approach was not fruitful.

Attempts to follow the reaction by NMR, using D_2O as solvent, were not successful. Other iron precursor was tested (iron (II) acetate), but the results were not conclusive.

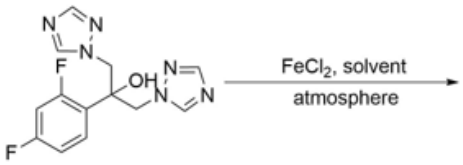

	Solvent	Atmosphere	
(a)	DCM/MeOH (2/1)	air	
(b)	MeOH	air	
(c)	D2O	air	
(d)	MeOH	air	$AgNO_3$
(e)	MeOH	inert	$AgNO_3$
(f)	DCM/MeOH (2/1)	inert	
(g)	MeOH	inert	

Figure 2.18- Summary of the fluconazole metalations performed with $FeCl_2$

The reactions (**f**) and (**g**) were a repetition of the two first reactions (**a** and **b**), but this time under nitrogen. The results were, nevertheless, identical. Given these outcomes, we

decided to utilize the reaction conditions defined in (**b**). The optimized conditions are described in the Scheme 2.11.

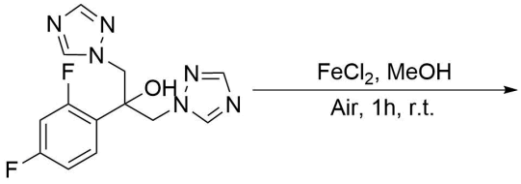

Scheme 2.11-Optimized conditions for the novel compound

To characterize the newly formed compound, an analysis through NMR spectroscopy and mass spectroscopy was performed.

By analyzing the ^{1}H NMR spectrum (Figure 2.19), an evident change of the signals in the left of the spectrum could be identified. These signals correspond to the hydrogen in the triazole ring. It can be concluded that the iron is coordinated with the nitrogen of the triazole ring.

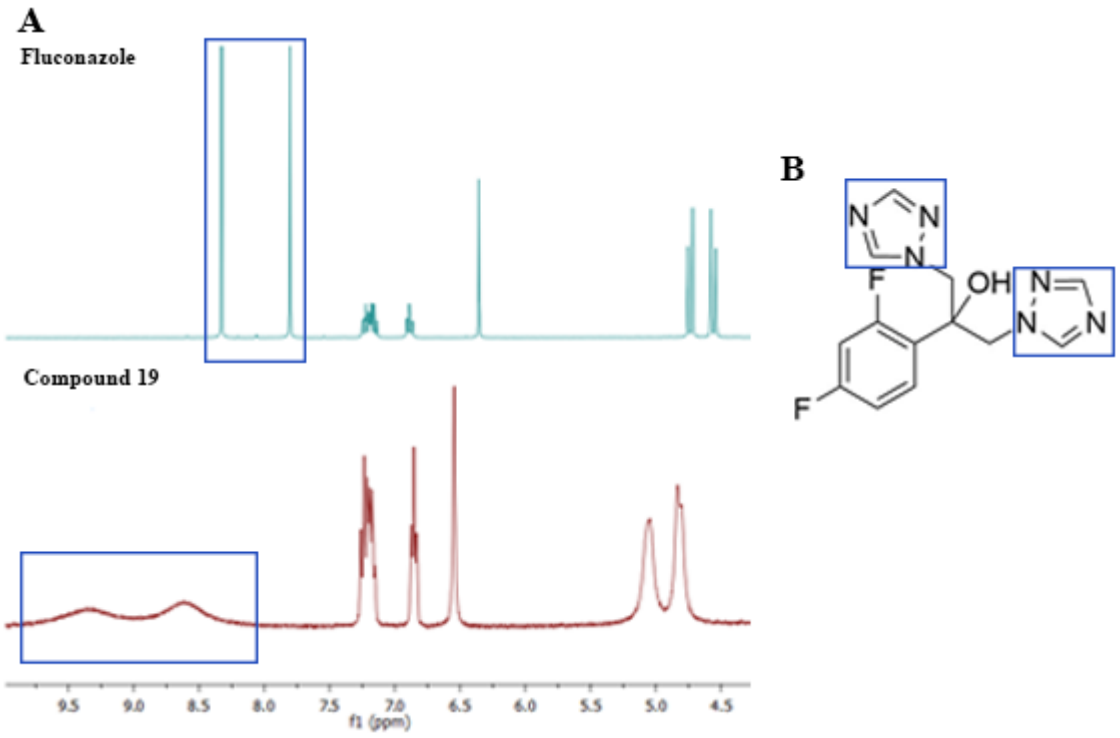

Figure 2.19-A: NMR spectrum of fluconazole and compound **19**. B: Fluconazole representation

The mass spectroscopy spectrum displays two peaks (Appendix Figure 7.1), one with 307 m/z corresponding to the fluconazole fragment that did not react or that underwent decoordination during measurement. The other peak has 667 m/z and it is most likely two

molecules of fluconazole and one iron (Figure 2.20), since the peak (667 m/z) presents the expected iron isotopic distribution.

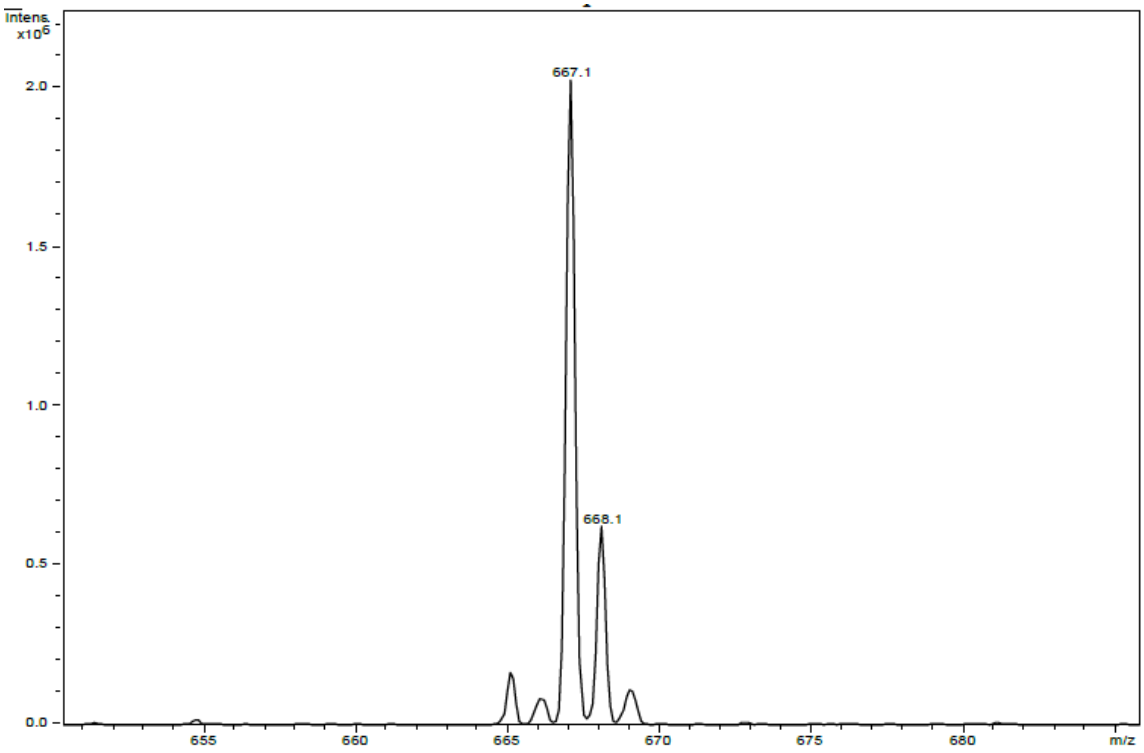

Figure 2.20-Mass spectroscopy spectrum of compound **19** (650-685 m/z)

After the analysis of all the spectrums and mass spectrometry results, it can be concluded that the compound formed in reaction (**b**) contained one molecule of Fe bounded to two molecules of fluconazole. Some possible structures for this compound are displayed in Figure 2.21. The analytical methods utilized to characterize the compound **19** were not sufficient to elucidate the structure of the compound. Attempts to obtain suitable crystals for X-Ray analysis were not successful.

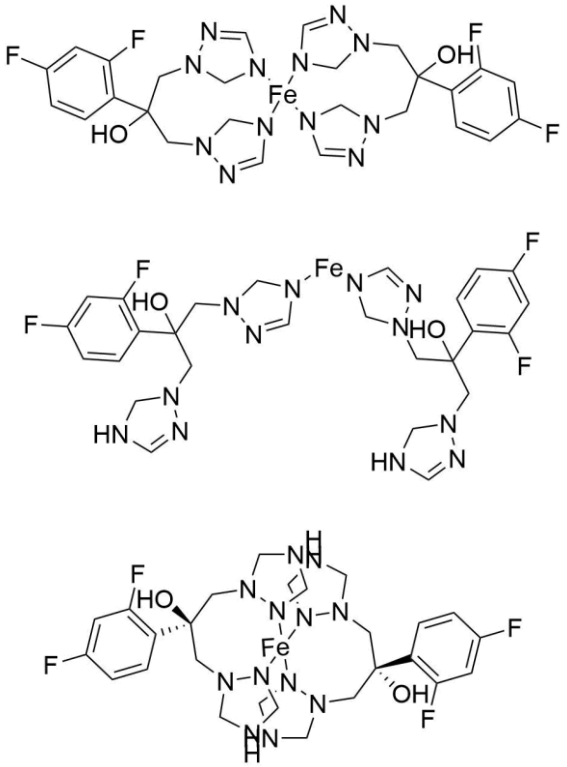

Figure 2.21-Possible structures of compound **19**

To purify the newly obtained compound, we performed a recrystallization in water. Crystal were readily formed, but ^{1}H NMR analysis of a sample indicated that it contained exclusively fluconazole. Thus, we conclude then the complex iron-fluconazole dissociates, when water.

2.7. Evaluation of the antifungal efficacy of the synthesized compounds against the yeasts *Saccharomyces cerevisiae* and *Candida glabrata*

The first tests were performed using *Saccharomyces cerevisiae* to understand the potential of each of the compounds (compounds **1**, **2** and **8**), at a very early stage of the project. Following this, all the derivatives of AZT and 5-FU synthesized (14 different compounds) were tested against *Candida glabrata*, one of the most highly opportunistic fungal pathogens.

2.7.1. Derivatives of AZT in *Saccharomyces cerevisiae*

The tests started with a first screen in *Saccharomyces cerevisiae* of three derivatives of AZT (Figure 2.22). Because concentrations of fluconazole equal or above 26 μM impair yeast growth[42], concentrations around and greater than this value were assayed to evaluate the antifungal activity of compounds **1**, **2** (27 and 81 μM) and **8** (20 and 59 μM).

The compounds were dissolved in DMSO (10 mg/ml) and the assay was performed in SC medium containing the drugs. Yeast cells were spotted onto the agar plates, incubated at 30ºC for 72 hours and growth was checked every 24 hours.

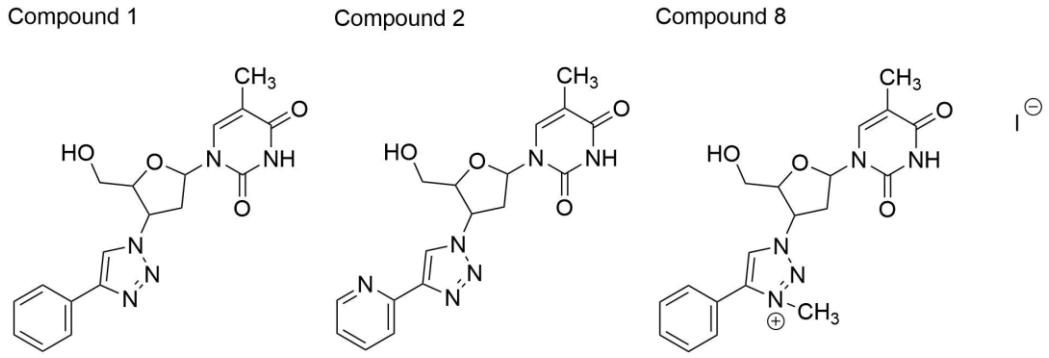

Figure 2.22-Tested compounds in *Saccharomyces cerevisiae*

The tests suggest that the antifungal activity of the novel compounds is very limited, when compared to that of fluconazole, since the yeast growth was not affected when the medium was supplemented with equimolar or higher concentrations of AZT derivatives (Figure 2.23).

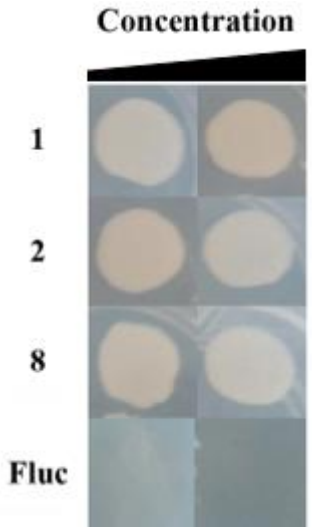

Figure 2.23- Antifungal activity of compounds **1**, **2** and **8** against *Saccharomyces cerevisiae*. Yeast cells were spotted onto SC agar medium. Growth was recorded after 48 hours. The tested concentrations were 27 and 81 µM (compounds **1** and **2**), 20 and 59 µM (compound **8**) and 26 and 52 µM (Fluconazol - Fluc).

To exclude any interference of the growth medium, we performed a similar assay, using YPD medium instead of SC. We observed no variations with respect to the SC tests (Figure 2.24).

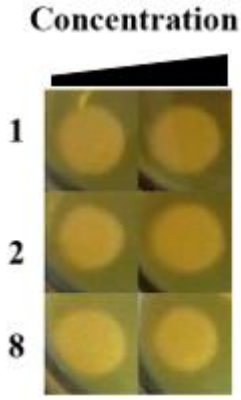

Figure 2.24- Antifungal activity of compounds **1**, **2** and **8** against *Saccharomyces cerevisiae* growing in YPD medium. Yeast cells were spotted onto YPD agar medium. Growth was recorded after 48 hours. The tested concentrations were 27 and 81 µM (compounds **1** and **2**), 20 and 59 µM (compound **8**).

We next assessed whether higher concentrations of the drugs would affect the yeast growth and found that only compound **8** exhibited fungistatic activity, when used at a concentration of 0.97 mM (Figure 2.25). Because DMSO *per se*, may be a stressor of yeast cells[43], to exclude the influence of the solvent in the compounds activities, we have also monitored yeast growth in medium treated with similar volumes of DMSO, but without the compound (mock control). DMSO did not appear to contribute to the fungistatic activity of compound **8** (Figure 2.25).

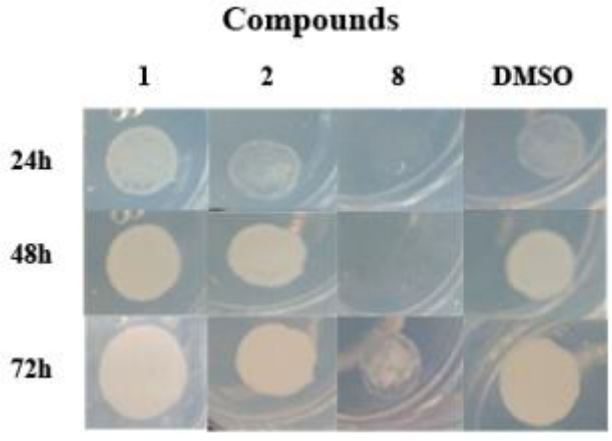

Figure 2.25- Antifungal activity of higher concentrations of compounds **1**, **2** and **8** against *Saccharomyces cerevisiae.* Yeast cells were spotted onto SC agar medium supplemented with 1.35 mM of compounds **1** and **2** or 0.97 mM of compound **8**. Growth was recorded after 24, 48 and 72h of incubation at 30ºC. DMSO was used as a mock control.

2.7.2. Derivatives of AZT in *Candida glabrata*

Two decades ago, *Candida albicans* dominated infections. Nowadays, this scenario has changed and *Candida glabrata* is the second most commonly isolated *Candida* species in the European Union and United States of America, demonstrating high incidence of resistance to azoles and echinocandins[8]. Thus, we decided to test the efficacy of AZT derivatives against *Candida glabrata*. To evaluate the antifungal activity of the synthesized compounds, we determined the minimal inhibitory concentration (MIC). The MIC value of an antifungal is the lowest concentration that results in ≤50% of reduction in the growth of the fungus, as compared to the control[44].

In the MIC determination procedure, drugs need to be sequentially diluted (1:2) in liquid growth media[45]. However, at higher concentrations the synthetized compounds precipitated after being added to the medium. Therefore, the solubility of all compounds was tested in water and in DMSO. The compounds with solubility lower than 2 mg/ml in water were dissolved in DMSO (compounds **1**-**7**). The remaining (triazolium salts) were dissolved directly in the medium (compounds **8**-**12**). Due to these solubility issues, the procedure for the preparation of the dilution of the compounds following the guidelines suggested by the CLSI document M27-A3[45] had to be adapted and the maximum concentration tested for each compound is listed in Table 2.1.

Table 2.1-Maximum concentration tested of AZT derivatives

Compound	Max concentration tested (mM)
1	1.35
2	1.35
3	0.62
4	1.25
5	0.68
7	2.50
8	5.86
9	3.70
10	2.63
11	1.95
12	4.62

None of the compounds affected the growth of *C. glabrata* (Figure 2.26), indicating that MICs should be well above the highest tested concentration (Table 2.1). Compound **8,** which had shown some activity against *Saccharomyces cerevisiae* (Figure 2.25), was ineffective against *C. glabrata*, even at higher concentrations.

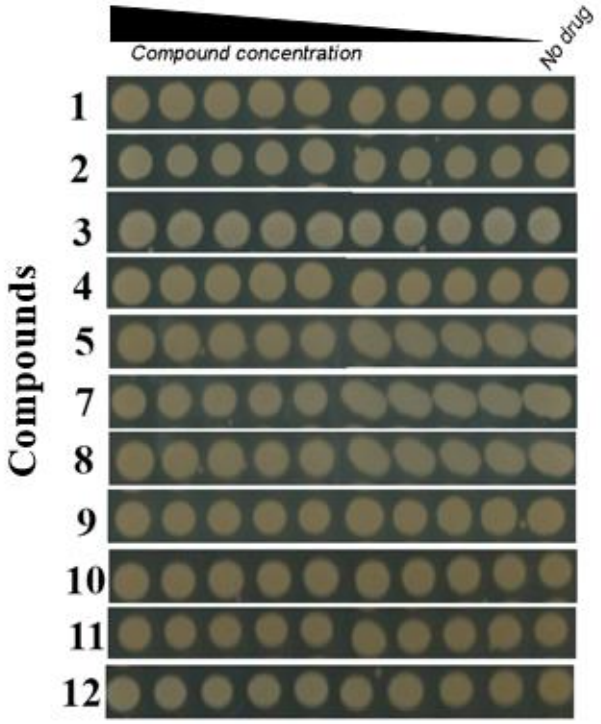

Figure 2.26- Antifungal activity of the AZT derivatives against *Candida glabrata*. The concentration range tested for each compound is listed in Table 3.1. Assays were performed as described in the *Experimental procedures* section.

2.7.3. Derivatives of 5-Fluorouracil in *Candida glabrata*

With the derivate compounds from 5-fluorouracil, solubility issues were also observed. As such, the procedure used for these compounds was similar to the one described above. The compounds with solubility lower than 1 mg/ml in water were dissolved in DMSO (compounds **16** and **17**). The remaining compound (a triazolium salt) was dissolved directly in medium (compound **18**). The maximum concentration tested from each compound is displayed in Table 2.2. The compounds in the tested concentrations did not seem to influence the growth of the yeast (Figure 2.27).

Table 2.2-Maximum concentration tested of 5-Fluorouracil derivatives

Compound	Max concentration tested (mM)
16	0.87
17	0.44
18	4.66

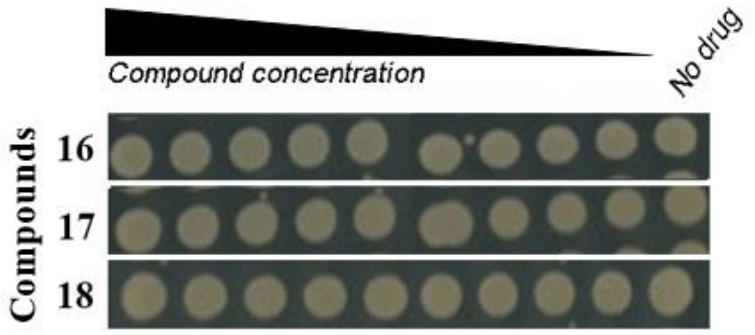

Figure 2.27- Antifungal activity of the 5-FC derivatives against *Candida glabrata*. The concentration range tested for each compound is listed in Table 3.1. Assays were performed as described in the *Experimental procedures* section.

It was not possible to calculate the *in vitro* MICs of the compounds. In fact, all the compounds appeared to not have any antifungal activity against *C. glabrata*, at least within the tested concentration range (Table 3.1). One possible cause for the lack of activity could be the fact that they were not able to bind to the iron in the active site of the enzyme lanosterol 14α-demethylase. One other reason could be that they could not be uptaken by the yeast cell.

3. Experimental procedures

All the chemicals were purchased from Sigma-Aldrich, TCI, Carbosynth, Honeywell and Carlo Erba and utilized without any further purification. The NMR spectra were recorded in the Magnetic Resonance Center António Xavier (CERMAX), using a Bruker AvanceII+ 400 MHz NMR spectrometer. Chemical shifts were measured in ppm (δ) relative to TMS (0.00 ppm). Coupling constants (*J*) are reported in Hertz (Hz). The following abbreviations describe the signal multiplicities: s (singlet), d (doublet), t (triplet), q (quartet) and m (multiplet). Chromatographic separations were performed using silica gel (230-400 Mesh) and for thin layer chromatography (TLC) Merck 60 F_{254} was utilized. Mass analyses data was obtained by the Mass Spectrometry Unit (UniMS), ITQB/iBET, Oeiras, Portugal.

3.1. Biological tests

3.1.1. Media conditions

YPD (1% yeast extract, 2% peptone, 2% dextrose). Synthetic complete (SC) medium (20% YNB, 20% CAA, 10% Glucose, 4% Ade, 2% Trp, 2% Ura). Roswell Park Memorial Institute (RPMI) 1640 medium (with glutamine and phenol red, but without bicarbonate). Solid plates contained 2% agar.

3.1.2. Susceptibility tests of *Saccharomyces cerevisiae*

Saccharomyces cerevisiae BY4742 cells (3 µl of a suspension of 0.1×10^7 cells/ml and 0.05×10^7 cells/ml) were spotted onto YPD or SC agar plates left untreated (control) or treated with compounds **1**, **2** (27, 81 and 1350 µM), **8** (20, 59 and 970 µM) or fluconazole (26 and 52 µM). Plates were next incubated at 30ºC for 72 hours. Every 24 hours, plates were examined to evaluate yeast growth. The growth of yeast cells in plates containing similar DMSO (the compounds solvent) concentrations were also tested (mock control).

3.1.3. Susceptibility tests of *Candida glabrata*

In vitro MICs of the compounds were evaluated in *Candida glabrata* HTL in 96-well microtest plates and according to the guidelines suggested by the CLSI document M27-A3[45]. The assays were performed in triplicate. Accordingly, microtest plates containing 100 µl of serial dilutions of the antifungal drugs in RPMI 1640 medium were inoculated with 100 µl of cells containing 0.2×10^7 cells/ml. The range of concentrations assayed is displayed in Table 3.1. After inoculation, plates were incubated at 37ºC for 48 hours. After 24h and 48h of incubation, 5 µl sample for each test mixture were taken, plated in solid RPMI 1640 medium and incubated at 37ºC. After 24 hours, the plates were examined to evaluate the degree of growth. The MIC of azoles was read as the lowest concentration that shown a decrease or an absence of growth, compared with the controls.

Table 3.1- Range of concentrations tested for compounds 1-5, 7-12 and 16-18

Compounds	Range of concentration tested (mM)
1	1.35-0.005
2	1.35-0.005
3	0.62-0.002
4	1.25-0.004
5	0.68-0.002
7	2.50-0.009
8	5.86-0.030
9	3.70-0.014
10	2.63-0.006
11	1.95-0.011
12	4.61-0.018
16	0.87-0.003
17	0.44-0.001
18	4.66-0.018

3.2. Synthetic procedures

Compound 1

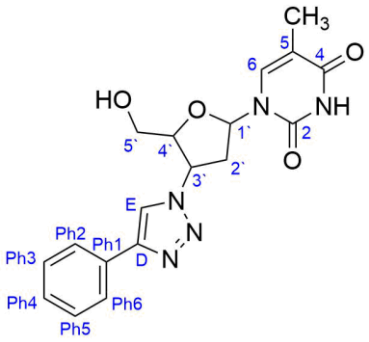

A suspension of 3`-azido-3`-deoxythymidine (800 mg, 3.00 mmol), phenylacetylene (395 µL, 3.60 mmol), $CuSO_4$ (29 mg, 0.18 mmol) and sodium ascorbate (357 mg, 1.80 mmol) in H_2O/tert-butanol (30 mL 1:1 v/v) was stirred at 100 ºC for 2 hours. After cooling the solid residue was filtered off and washed with Et_2O. The product was then purified by silica gel chromatography ($CHCl_3$: MeOH 10:1 v/v). Compound **1** was obtained as a white powder (922 mg, 83%).

^{1}H NMR (400 MHz, DMSO-d_6) δ 11.38 (1H, s, NH), 8.79 (1H, s, H_E), 7.90 – 7.81 (3H, m, H_6, H_{Ph2} and H_{Ph6}), 7.47 (2H, t, $^3J_{HH}$ = 8.0 Hz, H_{Ph3} and H_{Ph5}), 7.36 (1H, t, $^3J_{HH}$ = 8.0 Hz, H_{Ph4}), 6.46 (1H, t, $^3J_{HH}$ = 8.0 Hz, $H_{1`}$), 5.41 (1H, q, $^3J_{HH}$ = 6.6 Hz, $H_{3`}$), 5.31 (1H, t, $^3J_{HH}$ = 6.0 Hz, OH), 4.29 (1H, q, $^3J_{HH}$ = 4.0 Hz, $H_{4`}$) 3.77 – 3.65 (2H, m, $H_{5`}$), 2.85 – 2.67 (2H, m, $H_{2`}$), 1.83 (3H, s, CH_3).

^{13}C {^{1}H} NMR (100 MHz, DMSO-d_6) δ 164.2 (s, C=O), 150.9 (s, C=O), 147.0 (s, C_D), 136.7 (s, C_6), 131.0 (s, C_{Ph1}), 129.4 (2C, s, C_{Ph3} and C_{Ph5}), 128.4 (s, C_{Ph4}), 125.6 (2C, s, C_{Ph2} and C_{Ph6}), 121.4 (s, C_E), 110.1 (s, C_5), 84.8 (s, $C_{4`}$), 84.3 (s, $C_{1`}$), 61.2 (s, $C_{5`}$), 59.8 (s, $C_{3`}$), 37.6 (s, $C_{2`}$), 12.7 (s, CH_3).

Compound 2

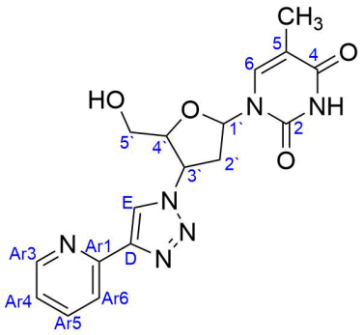

A suspension of 3`-azido-3`-deoxythymidine (800 mg, 3.00 mmol), 2-ethynylpyridine (360 µL, 3.60 mmol), $CuSO_4$ (29 mg, 0.18 mmol) and sodium ascorbate (357 mg, 1.80 mmol) in tert-butanol (20 mL) was stirred at 100 ºC for 2 hours. After cooling the solid residue was filtered off and washed with Et_2O. The solid residue was purified by silica gel chromatography ($CHCl_3$: MeOH 10:1 v/v). Compound **2** was obtained as a brown powder (560 mg, 50%).

^{1}H NMR (400 MHz, DMSO-d_6) δ 11.37 (1H, s, NH), 8.84 (1H, s, H_E), 8.62 (1H, d, $^3J_{HH}$ = 4.0 Hz, H_{Ar3}), 8.06 (1H, d, $^3J_{HH}$ = 8.0 Hz, H_{Ar6}), 7.92 (1H, m, H_{Ar4}), 7.85 (1H, s, H_6), 7.37 (1H, m, H_{Ar5}), 6.47 (1H, t, $^3J_{HH}$ = 6.0 Hz, $H_{1`}$), 5.41 (1H, q, $^3J_{HH}$ = 6.6 Hz, $H_{3`}$), 5.30 (1H, t, $^3J_{HH}$ = 4.0 Hz, OH), 4.30 (1H, q, $^3J_{HH}$ = 4.0 Hz, $H_{4`}$), 3.75 – 3.640 (2H, m, $H_{5`}$), 2.87 – 2.65 (2H, m, $H_{2`}$), 1.83 (3H, s, CH_3).

^{13}C {^{1}H} NMR (100 MHz, DMSO-d_6) δ 164.2 (s, C=O), 151.7 (s, C=O), 150.1 (d, J = 15.1 Hz, C_{Ar3}), 147.9 (s, C_D), 137.7 (s, C_{Ar4}), 136.7 (s, C_6), 123.5 (s, C_{Ar5}), 123.4 (s, C_E), 119.9 (s, C_{Ar6}), 110.1 (s, C_5), 84.8 (s, $C_{4`}$), 84.3 (s, $C_{1`}$), 79.6 (s, C_{Ar1}) 61.2 (s, $C_{5`}$), 59.8 (s, $C_{3`}$), 37.6 (s, $C_{2`}$), 12.7 (s, CH_3).

Compound 3

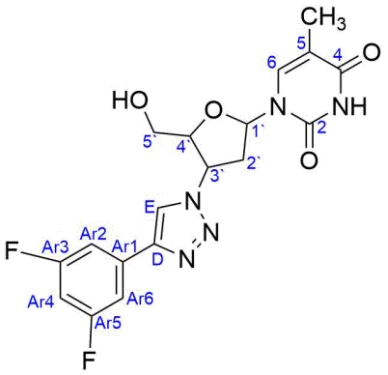

A suspension of 3`-azido-3`-deoxythymidine (300 mg, 1.13 mmol), 1-ethynyl-3,5-difluorobenzene (159 µL, 1.35 mmol), $CuSO_4$ (10.7 mg, 0.068 mmol) and sodium ascorbate (138 mg, 0.68 mmol) in tert-butanol (18 mL) was stirred at 100 ºC for 2 hours. After cooling the solid residue was filtered off and washed with Et_2O. The solid residue was purified by silica gel chromatography (DCM:MeOH 10:1 v/v). Compound **3** was obtained as a white powder (436 mg, 95%).

^{1}H NMR (400 MHz, DMSO-*d*$_6$) δ 11.38 (1H, s, NH), 8.94 (1H, s, H_E), 7.84 (1H, s, H_6), 7.58 (2H, d, $^3J_{HH}$ = 4.0 Hz, H_{Ar2} and H_{Ar6}), 7.25 (1H, t, $^3J_{HH}$ = 10.0 Hz, H_{Ar4}), 6.45 (1H, t, $^3J_{HH}$ = 8.0 Hz, $H_{1`}$), 5.42 (1H, q, $^3J_{HH}$ = 5.3 Hz, $H_{3`}$), 5.32 (1H, t, $^3J_{HH}$ = 4.0 Hz, OH), 4.28 (1H, q, $^3J_{HH}$ = 4.0 Hz, $H_{4`}$), 3.77-3.65 (2H, m, $H_{5`}$) , 2.83-2.68 (2H, m, $H_{2`}$), 1.83 (3H, s, CH_3).

^{13}C {^{1}H} NMR (100 MHz, DMSO-*d*$_6$) δ 164.1 (s, C=O), 150.9 (s, C=O), 145.0 (s, C_D), 136.6 (s, C_6), 122.8 (s, C_E), 110.1 (s, C_5), 108.5 (2C, d, *J* = 27.0 Hz, C_{Ar2} and C_{Ar6}), 103,7 (s, C_{Ar4}) 84.8 (s, $C_{4`}$), 84.3 (s, $C_{1`}$), 61.2 (s, $C_{5`}$), 60.1 (s, $C_{3`}$), 37.5 (s, $C_{2`}$), 12.7 (s, CH_3).

Compound 4

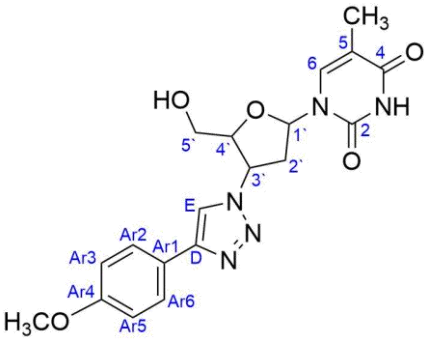

A suspension of 3`-azido-3`-deoxythymidine (300 mg, 1.13 mmol), ethynylanisole (178 mg, 1.35 mmol), $CuSO_4$ (10.7 mg, 0.067 mmol) and sodium ascorbate (138 mg, 0.68 mmol) in tert-butanol (15 mL) was stirred at 90 ºC for 2 hours. After cooling the solid residue was filtered off and washed with Et_2O. The solid residue was purified by silica gel chromatography (DCM:MeOH 10:1 v/v). Compound **4** was obtained as a white powder (102 mg, 22.8%).

^{1}H NMR (400 MHz, DMSO-*d*$_6$) δ 11.37 (1H, s, NH), 8.67 (1H, s, H_E), 7.85 (1H, s, H_6), 7.785 (2H, d, $^3J_{HH}$ = 12.0 Hz, H_{Ar3} and H_{Ar5}), 7.045 (2H, d, $^3J_{HH}$ = 12.0 Hz, H_{Ar2} and H_{Ar6}), 6.45 (1H, t, $^3J_{HH}$ = 8.0 Hz, $H_{1`}$), 5.39 (1H, q, $^3J_{HH}$ = 6.6 Hz, $H_{3`}$), 5.30, (1H, t, $^3J_{HH}$ = 6.0 Hz, OH) 4.28 (1H, q, $^3J_{HH}$ = 5.3 Hz, $H_{4`}$), 3.81 (3H, s, O-$CH_3$), 3.77-3.64 (2H, m, $H_{5`}$), 2.83-2.66 (2H, m, $H_{2`}$), 1.83 (3H, s, CH_3).

^{13}C {^{1}H} NMR (100 MHz, DMSO-*d*$_6$) δ 164.2 (s, C=O), 159.5 (s, C_{Ar4}), 150.9(s, C=O), 146.9 (s, C_D), 136.7 (s, C_6), 126.9 (s, C_{Ar3} and C_{Ar5}), 123.6 (s, C_{Ar1}), 120.4 (s, C_E), 114.8 (s, C_{Ar2} and C_{Ar6}), 110.1 (s, C_5), 84.8 (s, $C_{4`}$), 84.3 (s, $C_{1`}$), 61.2 (s, $C_{5`}$), 59.7 (s, $C_{3`}$), 55.6 (s, O-CH_3), 37.6 (s, $C_{2`}$), 12.7 (s, CH_3).

Compound 5

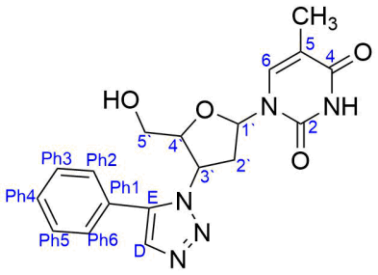

3`-azido-3`-deoxythymidine (100 mg, 0.37 mmol), phenylacetylene (80 µl, 0.75 mmol), and Cp*RuCl(PPh_3)$_2$ (0.05 eq.) were dissolved in dioxane (2 ml) under N_2 atmosphere, the resulting mixture stirred at 80ºC for 48 hours. After cooling the solvent were then removed under reduced pressure and the solid residue was purified by silica gel chromatography (DCM:MeOH 10:1 v/v). Compound **5** was obtained as a brown powder (116 mg, 85.5%).

^{1}H NMR (400 MHz, DMSO-*d*$_6$) δ 11.36 (1H, s, NH), 7.92 (1H, s, H_D), 7.78 (1H, s, H_6), 7.60-7.53, (5H, m, H_{Ph2}, H_{Ph3}, H_{Ph4}, H_{Ph5} and H_{Ph6}), 6.57 (1H, t, $^3J_{HH}$ = 8.0 Hz, $H_{1`}$), 5.25 (1H, t, $^3J_{HH}$ = 4.0 Hz, OH), 5.19-5.15 (1H, m, $H_{3`}$), 4.40 (1H, q, $^3J_{HH}$ = 4.0 Hz, $H_{4`}$), 3.63-3.47 (2H, m, $H_{5`}$), 2.66-2.57 (2H, m, $H_{2`}$), 1.78 (3H, s, CH_3).

^{13}C {^{1}H} NMR (100 MHz, DMSO-*d*$_6$) δ 164.1 (s, C=O), 150.9 (s, C=O), 138.3 (s, C_E), 136.5 (s, C_6), 133.3 (s, C_D), 129.6 (5C, d, C_{Ph2}, C_{Ph3}, C_{Ph4}, C_{Ph5} and C_{Ph6}), 126.8 (s, C_{Ph1}), 110.1 (s, C_5), 85.3 (s, $C_{4`}$), 85.1 (s, $C_{1`}$), 61.8 (s, $C_{5`}$), 58.1 (s, $C_{3`}$) 38.1 (s, $C_{2`}$), 12.7 (s, CH_3).

Compound 6

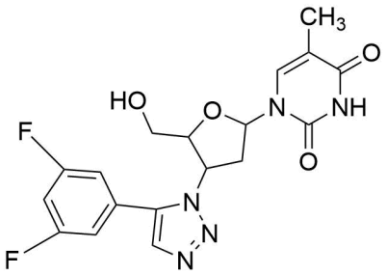

3`-azido-3`-deoxythymidine (100 mg, 0.37 mmol), 1-ethynyl-3,5-difluorobenzene (90 µl, 0.75 mmol), and Cp*RuCl(PPh_3)$_2$ (0.05 eq.) were dissolved in dioxane (5 ml) under N_2 atmosphere, the resulting mixture stirred at 80ºC for 48 hours. After cooling the solvent were then removed under reduced pressure and the solid residue was purified by silica gel chromatography (DCM:MeOH 10:1 v/v). The final product was not isolated.

Compound 7

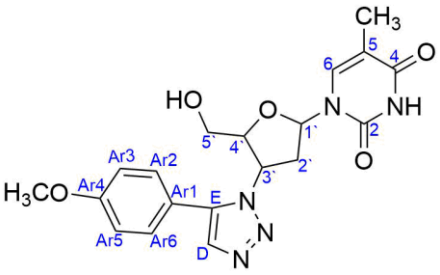

3`-azido-3`-deoxythymidine (200 mg, 0.75 mmol), ethynylanisole (198 mg, 1.50 mmol), and Cp*RuCl(PPh_3)$_2$ (0.05 eq.) were dissolved in dioxane (10 ml) under N_2 atmosphere, the resulting mixture stirred at 80ºC for 48 hours. After cooling the solvent were then removed under reduced pressure and the solid residue was purified by silica gel chromatography (DCM:MeOH 10:1 v/v). Compound **7** was obtained as a brown powder (259 mg, 86.7%).

^{1}H NMR (400 MHz, DMSO-*d*$_6$) δ 11.36 (1H, s, NH), 7.85 (1H, s, H_D), 7.79 (1H, s, H_6), 7.47 (2H, d, $^3J_{HH}$ = 8.0 Hz, H_{Ar3} and H_{Ar5}), 7.12 (2H, d, $^3J_{HH}$ = 8.0 Hz, H_{Ar2} and H_{Ar6}), 6.57 (1H, t, $^3J_{HH}$ = 4.0 Hz, $H_{1`}$), 5.25 (1H, t, $^3J_{HH}$ = 4.0 Hz, OH), 5.16-5.14 (1H, m, $H_{3`}$), 4.38 (1H, q, $^3J_{HH}$ = 2.6 Hz, $H_{4`}$), 3.83 (3H, s, O-$CH_3$), 3.63-3.49 (2H, m, $H_{5`}$), 2.62-2.51 (2H, m, $H_{2`}$), 1.79 (3H, s, CH_3).

^{13}C {^{1}H} NMR (100 MHz, DMSO-*d*$_6$) δ 164.1 (s, C=O), 160.6 (s, C_{Ar4}), 150.9 (s, C=O), 138.1 (s, C_E), 136.5 (s, C_6), 133.1 (s, C_D), 131.1 (2C, s, C_{Ar3} and C_{Ar5}), 118.7 (s, C_{Ar1}), 115.0 (2C, s, C_{Ar2} and C_{Ar6}), 110.1 (s, C_5), 85.3 (s, $C_{4`}$), 85.1 (s, $C_{1`}$), 61.8 (s, $C_{5`}$), 58.6 (s, $C_{3`}$), 55.7 (s, O-CH_3), 38.2 (s, $C_{2`}$), 12.7 (s, CH_3).

Compound 8

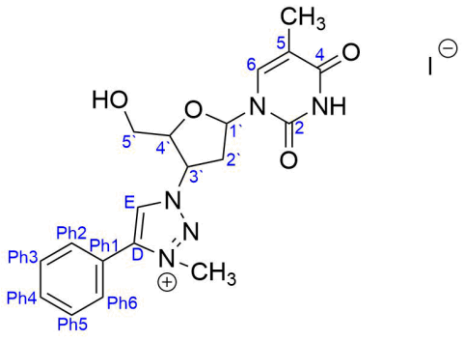

To a suspension of Compound **1** (200 mg, 0.54 mmol) in DMF (12 mL), was added iodomethane (337 µL, 5.40 mmol) and stirred at 100 ºC for 24 hours. Then, after cooling, Et_2O was added to precipitate the compound and the solvent was taken out. The final product washed with more Et_2O. Compound **8** was obtained as a yellow powder (201 mg, 72.8%).

^{1}H NMR (400 MHz, DMSO-*d*$_6$) δ 11.42 (1H, s, NH), 9.37 (1H, s, H_E), 7.82 (1H, s, H_6), 7.78 – 7.76 (2H, m, H_{Ph2} and H_{Ph6}), 7.71-7.69 (3H, m, H_{Ph3} and H_{Ph4} and H_{Ph5}), 6.45 (1H, t, $^3J_{HH}$ = 8.0 Hz, $H_{1`}$), 5.67 (1H, m, $H_{3`}$), 5.43 (1H, t, $^3J_{HH}$ = 6.0 Hz, OH) 4.47 (1H, q, $^3J_{HH}$ = 4.0 Hz, $H_{4`}$), 4.34 (3H, s, N-$CH_3$), 3.79-3.76 (2H, m, $H_{5`}$), 2.975 – 2.79 (2H, m, $H_{2`}$), 1.83 (3H, s, CH_3).

^{13}C {^{1}H} NMR (100 MHz, DMSO-*d*$_6$) δ 164.1 (s, C=O), 150.9 (s, C=O), 142.9 (s, C_D), 136.6 (s, C_6), 132.0 (s, C_{Ph4}),129.9 (2C, s, C_{Ph3} and C_{Ph5}) 129.7 (2C, s, C_{Ph2} and C_{Ph6}), 129.1 (s, C_E), 123.0 (s, C_{Ph1}), 110.3 (s, C_5), 84.4 (s, $C_{1`}$), 84.0 (s, $C_{4`}$), 64.0 (s, $C_{3`}$), 61.1 (s, $C_{5`}$),39.3 (s, N-CH_3) 37.0 (s, $C_{2`}$), 12.7 (s, CH_3).

Compound 9

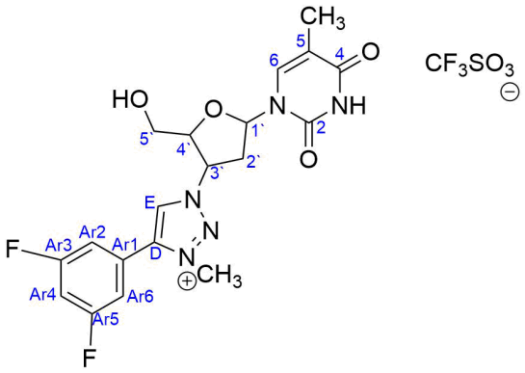

Compound **3** (90 mg, 0.22 mmol) was dissolved in DMF (2.5 ml) under N_2 atmosphere and was added Mehtyl trifluoromethanesulfonate (75 µL, 0.69 mmol) and stirred at 100 ºC overnight. Then, after cooling, Et_2O was added to precipitate the compound and the solvent was taken out. The final product washed with more Et_2O. Compound **9** was obtained as a brown powder (10 mg, 8%).

^{1}H NMR (400 MHz, DMSO-*d*$_6$) δ 11.41 (1H, s, NH), 9.41 (1H, s, H_E), 7.81 (1H, s, H_6), 7.68 (1H, t, $^3J_{HH}$ = 8.0 Hz, H_{Ar4}), 7.595 (2H, d, $^3J_{HH}$ = 4.0 Hz, H_{Ar2} and H_{Ar6}), 6.46-6.42 (1H, m, $H_{1`}$), 5.70-5.66 (1H, m, $H_{3`}$), 4.47-4.44 (2H, m, $H_{4`}$), 4.38 (3H, s, N-$CH_3$), 3.81-3.73 (2H, m, $H_{5`}$), 2.98-2.79 (2H, m, $H_{2`}$), 1.83 (3H, s, CH_3).

^{13}C {^{1}H} NMR (100 MHz, DMSO-*d*$_6$) δ 164.1 (s, C=O), 150.9 (s, C=O), 140.7 (s, C_D), 136.6 (s, C_6), 130.0 (s, C_E), 110.3 (s, C_5), 113.6 (2C, d, *J* = 20 Hz, C_{Ar2} and C_{Ar6}), 107,7 (s, C_{Ar4}) 84.4 (s, $C_{1`}$), 64.2 (s, $C_{3`}$), 62.9 (s, $C_{4`}$), 61.1 (s, $C_{5`}$) 39.4 (s, N-CH_3) , 34.8 (s, $C_{2`}$), 12.7 (s, CH_3).

Compound 10

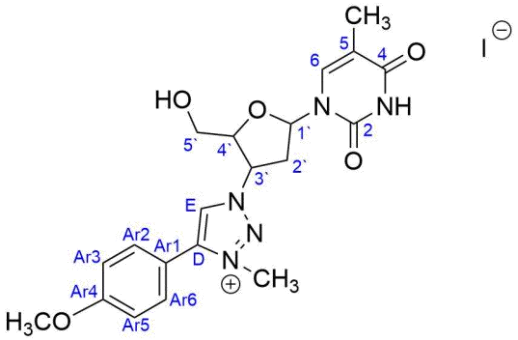

Compound **4** (73 mg, 0.18 mmol) was dissolved in DMF (5 ml) and was added iodomethane (114 µL, 1.8 mmol) and stirred at 100 ºC for 24 hours. Then, after cooling, Et_2O was added to precipitate the compound and the solvent was taken out. The final product washed with more Et_2O. Compound **10** was obtained as a brown powder (31 mg, 31.3%).

^{1}H NMR (400 MHz, DMSO-*d*$_6$) δ 11.40 (1H, s, NH), 9.31 (1H, s, H_E), 7.83 (1H, s, H_6), 7.71 (2H, d, $^3J_{HH}$ = 8.0 Hz, H_{Ar3} H_{Ar5}), 7.23 (2H, d, $^3J_{HH}$ = 8.0 Hz, H_{Ar2} and H_{Ar6}), 6.44 (1H, t, $^3J_{HH}$ = 8.0 Hz, $H_{1`}$), 5.68-5.63 (1H, m, $H_{3`}$), 4.49-4.46 (1H, m, $H_{4`}$), 4.30 (3H, s, N-$CH_3$), 3.87 (3H, s, O-$CH_3$), 3.79-3.77 (2H, m, $H_{5`}$), 2.94-2.79 (2H, m, $H_{2`}$), 1.82 (3H, s, CH_3).

^{13}C {^{1}H} NMR (100 MHz, DMSO-*d*$_6$) δ 164.1 (s, C=O), 162.0 (s, C_{Ar4}), 150.8 (s, C=O), 142.8 (s, C_D), 136.6 (s, C_6), 131.4 (s, C_{Ar3} and C_{Ar5}), 128.6 (s, C_E), 115.4 (s, C_{Ar2} and C_{Ar6}), 114.9 (s, C_{Ar1}), 110.3 (s, C_5), 84.4 (s, $C_{1`}$), 84.0 (s, $C_{4`}$), 63.9 (s, $C_{3`}$), 61.1 (s, $C_{5`}$), 56.0 (s, O-CH_3), 39.2 (s, N-CH_3), 37.0 (s, $C_{2`}$),12.7 (s, CH_3).

Compound 11

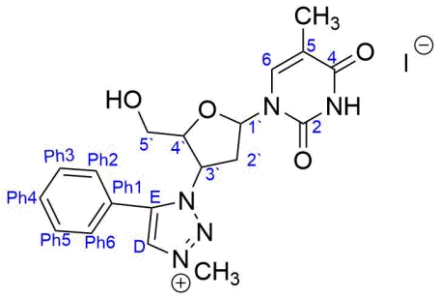

Compound **5** (50 mg, 0.14 mmol) was dissolved in DMF (3.5 ml) and was added iodomethane (85 µL, 1.4 mmol) and stirred at 100 ºC for 24 hours. Then, after cooling, Et_2O was added to precipitate the compound and the solvent was taken out. The final product washed with more Et_2O. Compound **11** was obtained as a brown powder (61 mg, 88.4%).

^{1}H NMR (400 MHz, DMSO-d_6) δ 11.39 (1H, s, NH), 9.12 (1H, s, H_D), 7.76 (1H, s, H_6), 7.72-7.66 (5H, m, H_{Ph2}, H_{Ph3}, H_{Ph4}, H_{Ph5} and H_{Ph6}), 6.45 (1H, t, $^3J_{HH}$ = 6.0 Hz, $H_{1`}$), 5.39-5.33 (1H, m, $H_{3`}$ and OH), 4.53-4.52 (2H, m, $H_{4`}$), 4.44 (3H, s, N-$CH_3$), 3.63-3.49 (2H, m, $H_{5`}$), 2.90-2.68 (2H, m, $H_{2`}$), 1.78 (3H, s, CH_3).

^{13}C {^{1}H} NMR (100 MHz, DMSO-d_6) δ 164.1 (s, C=O), 150.8 (s, C=O), 143.0 (s, C_E), 136.4 (s, C_6), 132.1 (s, C_{Ph1}), 130.6 (s, C_D), 130.2 (5C, d, C_{Ph2}, C_{Ph3}, C_{Ph4}, C_{Ph5} and C_{Ph6}), 122.7 (s, C_{Ph4}), 110.3 (s, C_5), 85.0 (s, $C_{1`}$), 84.5 (s, $C_{4`}$), 62.5 (s, $C_{3`}$), 61.5 (s, $C_{5`}$), 40.7 (s, N-CH_3), 37.6 (s, $C_{2`}$), 12.7 (s, CH_3).

Compound 12

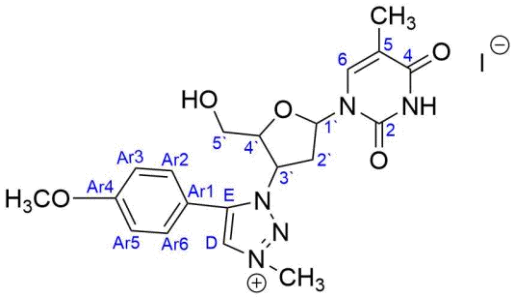

Compound **7** (42 mg, 0.11 mmol) was dissolved in DMF (2 ml) and was added iodomethane (65 µL, 1.1 mmol) and stirred at 100 ºC for 24 hours. Then, after cooling, Et_2O was added to precipitate the compound and the solvent was taken out. The final product washed with more Et_2O. Compound **12** was obtained as a brown powder (44 mg, 77.9%).

^{1}H NMR (400 MHz, DMSO-*d*$_6$) δ 11.40 (1H, s, NH), 9.05 (1H, s, H_D), 7.77 (1H, s, H_6), 7.59 (2H, d, $^3J_{HH}$ = 6.0 Hz, H_{Ar3} and H_{Ar5}), 7.24 (2H, d, $^3J_{HH}$ = 6.0 Hz, H_{Ar2} and H_{Ar6}) 6.44 (1H, t, $^3J_{HH}$ = 8.0 Hz, $H_{1`}$), 5.39-5.34 (1H, m, $H_{3`}$and OH), 4.515 (1H, q, $^3J_{HH}$ = 4.0 Hz, $H_{4`}$), 4.42 (3H, s, N-$CH_3$), 3.88 (3H, s, O-$CH_3$), 3.64-3.51 (2H, m, $H_{5`}$), 2.87-2.65 (2H, m, $H_{2`}$), 1.78 (3H, s, CH_3).

^{13}C {^{1}H} NMR (100 MHz, DMSO-*d*$_6$) δ 164.1 (s, C=O), 162.0 (s, C_{Ar4}), 150.8 (s, C=O), 143.0 (s, C_E), 136.4 (s, C_6), 132.0 (2C, s, C_{Ar3} and C_{Ar5}), 130.3 (s, C_D), 115.5 (2C, s, C_{Ar2} and C_{Ar6}), 114.5 (s, C_{Ar1}), 110.3 (s, C_5), 85.0 (s, $C_{1`}$), 84.5 (s, $C_{4`}$), 62.3 (s, $C_{3`}$), 61.6 (s, $C_{5`}$), 56.0 (s, O-CH_3), 40.6 (s, N-CH_3), 37.6 (s, $C_{2`}$), 12.7 (s, CH_3).

Compound 13

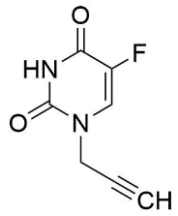

5FU (600 mg, 4.62 mmol) together with 1,8-diazabicyclo[5.4.0]undec-7-ene (820 µl, 5.40 mmol) were dissolved in dry DMF (6 ml) under N_2 atmosphere and cooled to 4 ºC. Propargyl bromide (500 µl, 4.62 mmol) was added dropwise to the mixture and the resulted stirred at room temperature overnight. The final product was precipitated with Et_2O, washed with both Et_2O and pentane and purified via silica gel chromatography (DCM). Compound **13** was obtained as a white powder (108 mg, 13.9%).

Compound 14

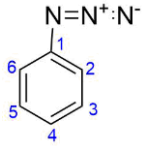

Aniline (1.55 ml, 1.70 mmol) was dissolved in 32 ml acetonitrile in a 250 ml round bottle and cooled in an ice bath. To this stirred solution was added *t*-BuONO (2.98 ml, 2.50 mmol) followed by $TMSN_3$ (2.63 ml, 2.00 mmol) dropwise. The mixture was stirred for 2 days at room temperature. The mixture was concentrated under vacuum and the solid residue purified by silica gel chromatography (Et_2O) to give a yellow oil (1.3 ml, 76.5%).

^1H NMR (400 MHz, DMSO-d_6) δ 7.43 (2H, t, $^3J_{HH}$ = 8.0 Hz, H_3 and H_5), 7.205 (1H, t, $^3J_{HH}$ = 6.0 Hz, H_4), 7.13 (2H, d, $^3J_{HH}$ = 8.0 Hz, H_2 and H_6).

^{13}C {^1H} NMR (100 MHz, DMSO-d_6) δ 139.7 (s, C_1), 130.4 (2C, s, C_3 and C_5), 125.6 (s, C_4), 119.5 (2C, s, C_2 and C_6).

Compound 15

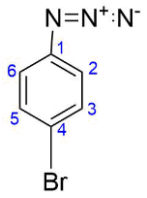

4-bromoaniline (2.92 ml, 1.70 mmol) was dissolved in 110 ml acetonitrile in a 250 ml round bottle and cooled in an ice bath. To this stirred solution was added *t*-BuONO (2.98 ml, 2.50 mmol) followed by $TMSN_3$ (2.63 ml, 2.00 mmol) dropwise. The mixture was stirred for 2 days at room temperature. The mixture was concentrated under vacuum and the solid residue purified by silica gel chromatography (Et_2O) to give an orange oil (1.45 ml, 75.4%)

^{1}H NMR (400 MHz, DMSO-d_6) δ 7.50 (2H, d, $^3J_{HH}$ = 8.0 Hz, H_3 and H_5), 7.01 (2H, d, $^3J_{HH}$ = 8.0 Hz, H_2 and H_6).

^{13}C {^{1}H} NMR (100 MHz, DMSO-d_6) δ 139.4 (s, C_1), 133.2 (2C, s, C_2 and C_6), 121.8 (2C, s, C_2 and C_6), 117.5 (s, C_4).

Compound 16

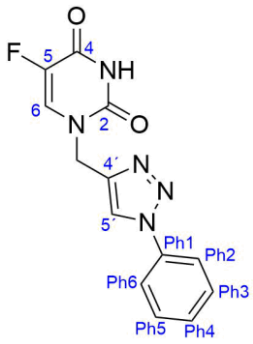

A suspension of compound **12** (176 mg, 1.05 mmol), compound **13** (147 µL, 1.26 mmol), $CuSO_4$ (10 mg, 0.063 mmol) and sodium ascorbate (125 mg, 0.63 mmol) in tert-butanol (10 mL) was stirred at 80 ºC for 26 hours. After cooling the solid residue was filtered off and washed with Et_2O. The solid residue was purified by silica gel chromatography ($CHCl_3$: MeOH 10:1 v/v). compound **16** was obtained as a white powder (108 mg, 36%).

^{1}H NMR (400 MHz, DMSO-*d*$_6$) δ 11.87 (1H, s, NH), 8.81 (1H, s, $H_{5`}$), 8.23 (1H, d, $^3J_{HF}$ = 8.0 Hz, H_6), 7.90 (2H, d, $^3J_{HH}$ = 8.0 Hz, H_{Ph2} and H_{Ph6}) 7.61 (2H, t, $^3J_{HH}$ = 6.0 Hz, H_{Ph3} and H_{Ph5}), 7.50 (1H, t, $^3J_{HH}$ = 8.0 Hz, H_{Ph4}), 5.01 (2H, s, CH_2).

^{13}C {^{1}H} NMR (100 MHz, DMSO-*d*$_6$) δ 157.9 (s, C=O), 149.9 (s, C=O), 144.0 (s, $C_{4`}$), 139.1 (s, $C_5$), 136.9 (1C, s, $C_{Ph1}$), 130.3 (3C, s, $C_6$, $C_{Ph3}$ and $C_{Ph5}$), 129.2 (1C, s, $C_{Ph4}$), 122.1 (s, $C_{5`}$), 120.4 (2C, s, C_{Ph2} and C_{Ph6}), 43.2 (s, CH_2).

Compound 17

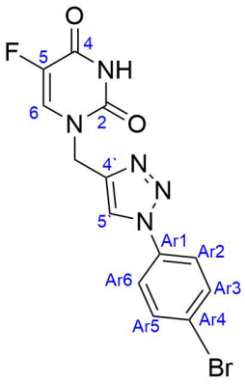

A suspension of compound **12** (100 mg, 0.59 mmol), compound **14** (80 µL, 0.71 mmol), $CuSO_4$ (11 mg, 0.071 mmol) and sodium ascorbate (141 mg, 0.71 mmol) in tert-butanol (10 mL) was stirred at 80 ºC for 28 hours. After cooling the solid residue was filtered off and washed with Et_2O. The solid residue was purified by silica gel chromatography ($CHCl_3$: MeOH 10:1 v/v). Compound **17** was obtained as a light brown powder (33 mg, 15%).

^{1}H NMR (400 MHz, DMSO-d_6) δ 11.89 (1H, s, NH), 8.84 (1H, s, $H_{5'}$), 8.23 (1H, d, $^3J_{HF}$ = 8.0 Hz, H_6), 7.88, (2H, d, $^3J_{HH}$ = 8.0 Hz, H_{Ar3} and H_{Ar5}), 7.81 (2H, d, $^3J_{HH}$ = 8.0 Hz, H_{Ar2} and H_{Ar6}), 5.01 (2H, s, CH_2).

^{13}C {^{1}H} NMR (100 MHz, DMSO-d_6) δ 158.1 (s, C=O), 149.9 (s, C=O), 136.1 (s, C_{Ar1}), 133.2 (2C, s, C_{Ar2} and C_{Ar6}), 130.5 (s, C_6), 122.4-121.8 (4C, m, $C_{5'}$, C_{Ar3}, C_{Ar4} and C_{Ar5}), 43.2 (s, CH_2).

Compound 18

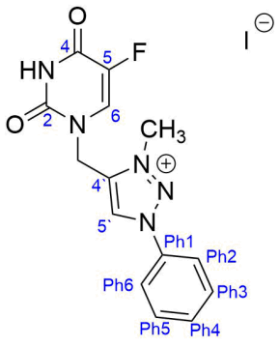

To a suspension of Compound **15** (80 mg, 0,28 mmol) in DMF (8 mL), was added iodomethane (52 µL, 0.83 mmol) and stirred at 100 ºC for 24 hours. Then, after cooling, Et_2O was added to precipitate the compound and the solvent was taken out. The final product washed with more Et_2O. Compound **18** was obtained as a yellow powder (55 mg, 46%).

^{1}H NMR (400 MHz, DMSO-*d*$_6$) δ 12.08 (1H, s, NH), 9.63 (1H, s, $H_{5`}$) 8.185 (1H, d, $^3J_{HF}$ = 4.0 Hz, H_6), 8.00-7.98 (2H, m, H_{Ph2} and H_{Ph6}), 7.75-7.76 (3H, m, H_{Ph3}, H_{Ph4} and H_{Ph5}), 5.27 (2H, s, CH_2), 4.46 (3H, s, N-CH_3).

^{13}C {^{1}H} NMR (100 MHz, DMSO-*d*$_6$) δ 158.1 (s, C=O), 150.1 (s, C=O), 141.7 (s, C-F), 140.8 (s, $C_{4`}$), 139.4 (s, C-F), 135.0 (s, $C_{Ph1}$), 132.3 ($C_{Ph4}$), 130.9 (2C, s, $C_{Ph3}$ and $C_{Ph5}$), 129.6 (d, J = Hz, $C_6$), 128.7 (s, $C_{5`}$), 121.7 (2C, s, C_{Ph2} and C_{Ph6}), 40.5 (s, N-CH_3), 39.0 (s, CH_2).

Compound 19

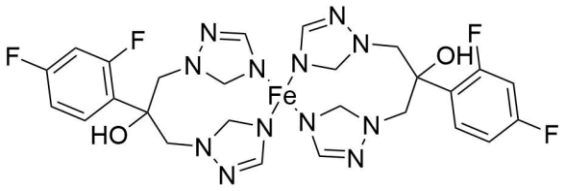

Fluconazole (153 mg, 0.5 mmol) was dissolved in MeOH (2 ml) under N_2 atmosphere. Afterwards $FeCl_2$ (63mg, 0.5 mmol) was dissolved in MeOH (5 ml) and added dropwise under N_2 atmosphere. The resulting mixture was stirred at room temperature for 1 hour. The final product was filtered off and washed with Et_2O (173 mg).

4. Conclusions

The synthesis of 1,4-disubstituted triazoles derived from AZT catalyzed by Cu(I) was successful. Compounds **1** and **3** were obtained with excellent yields (83% and 95% respectively), while the yield of compound **2** and **4** was moderate (50% and 33% respectively).

The synthesis of 1,5-disubstituted triazoles derived from AZT catalyzed by ruthenium was employed. Compounds **5** and **7** were obtained with excellent yields (85.5% and 86.7% respectively), compound **6** was synthesized as well, but the purification was not successful.

Methylation of 1,4 and 1,5-disubstituted triazoles was performed with methyliodide. For compound **9**, a stronger methylating agent (methyltriflate) was required. Compounds **8**, **11** and **12** were obtained with good yields (72.8%, 88.4% and 77.9% respectively), while for compound **9** and **10** yields were lower (8% and 33% respectively).

Synthetic procedure for the alkynylation of 5-fluorouracil to obtain compound **13** was employed successfully, although with very low yield (13%).

The synthesis of 1,4-disubstituted triazoles from 5-Fluorouracil catalyzed by Cu(I) was performed, obtaining compound **16**, and compound **17** in moderate yields (36% and 15% respectively). Methylation of compound **16** was successfully employed to obtain the corresponding compound **18** with 46% yield.

Compound **8** was reacted with silver oxide. ^{1}H NMR spectroscopy confirmed the formation of a new compound, presumably a silver NHC, with a spectroscopic yield of 55%. Attempts to increase the yield of the reaction were ineffective.

Coordination of fluconazole to iron was successfully achieved. Mass spectroscopy measurements indicate that the new compound contains two fluconazole units per metal center. Stability studies in aqueous media indicate that the compound is not stable.

In the biological tests against *S. cerevisiae*, only compound **8** showed capacity to decrease the proliferation rate of the yeast, for a concentration of 0.97 mM.

Regarding the tests against *Candida glabrata*, the compounds did not demonstrate any influence in the growth of this fungus. It can be concluded that the synthesized triazoles, in the concentrations tested for the MIC determination, did not have any antifungal activity against *Candida glabrata.*

5. Future work

As future lines of work, the modification of the synthetic strategy to achieve more active compounds should be pursued. Specifically, we will focus on solubility aspects, due to the difficulty observed in the solubilization of the compounds.

The metallation of compounds should be investigated as well, since our preliminary results indicate that formation of silver NHC complexes can be achieved.

Molecular docking studies to design, and later to synthesize, new compounds that better interact with the desired enzyme should be pursued.

Finally, these compounds will be tested to determine their antiviral activity

6. Bibliography

(1) Lupetti, A.; Danesi, R.; Campa, M.; Tacca, M. Del; Kelly, S. *Trends Mol. Med.* **2002**, *8* (2), 76–81.

(2) Zhu, L.; Brassard, C. J.; Zhang, X.; Guha, P. M.; Clark, R. J. *Chem. Rec.* **2016**, *16* (I), 1501–1517.

(3) Johansson, J. R.; Beke-Somfai, T.; Said Stålsmeden, A.; Kann, N. *Chem. Rev.* **2016**, *116* (23), 14726–14768.

(4) Willey, J. M.; Sherwood, L. M.; Woolverton, C. J. *Prescott's Principles of Microbiology*; 2009.

(5) Chen, A.; Sobel, J. D. *Expert Opin. Emerg. Drugs* **2005**, *10* (1), 21–33.

(6) Robbins, N.; Wright, G. D.; Cowen, L. E. *Microbiol. Spectr.* **2016**, *4* (5), 1–20.

(7) Canuto, M. M.; Rodero, F. G. *Lancet Infect. Dis.* **2002**, *2* (9), 550–563.

(8) Denning, D. W.; Bromley, M. J. *Science (80-.).* **2015**, *347* (6229), 1414–1416.

(9) Enoch, D. A.; Yang, H.; Aliyu, S. H.; Micallef, C. In *Human Fungal Pathogen Identication*; 2017; pp 17–65.

(10) Loeffler, J.; Stevens, D. A. **2003**, *36* (Suppl 1), 31–41.

(11) Ashley, E. S. D.; Lewis, R.; Lewis, J. S.; Martin, C.; Andes, D. *Clin. Infect. Dis.* **2006**, *43* (Suppl 1), S28–S39.

(12) Lewis, R. E. *Mayo Clin. Proc.* **2011**, *86* (8), 805–817.

(13) Shapiro, R. S.; Robbins, N.; Cowen, L. E. *Microbiol. Mol. Biol. Rev.* **2011**, *75* (2), 213–267.

(14) Owens, J. N.; Skelley, J. W.; Kyle, J. A. *US Pharm. 35(8)* **2010**, *35* (8), 44–56.

(15) Johnson, M. D.; Perfect, J. R. *Curr. Fungal Infect. Rep.* **2010**, *4* (2), 87–95.

(16) Ghannoum, M. A.; Rice, L. B. *Clin. Microbiol. Rev.* **1999**, *12* (4), 501–517.

(17) Bell, A. S. In *Comprehensive Medical Chemistry II*; 2006; Vol. 7, pp 445–468.

(18) Denning, D. W. *Lancet* **2003**, *362* (9390), 1142–1151.

(19) Sheehan, D. J.; Hitchcock, C. a.; Sibley, C. M. *Clin. Microbiol. Rev.* **1999**, *12* (1), 40–79.

(20) Zhang, A. Y.; Camp, W. L.; Elewski, B. E. *Dermatol. Clin.* **2007**, *25* (2), 165–183.

(21) Maertens, J. A. *Clin. Microbiol. Infect.* **2004**, *10* (Suppl. 1), 1–10.

(22) Vermes, A.; Guchelaar, H. J.; Dankert, J. *J ournal Antimicrob. Chemother.* **2000**, *46* (2), 171–179.

(23) Chandra, J.; Mohammad, S.; Ghannoum, M. A. In *Antimicrobial Drug Resistance*; 2009; pp 313–326.

(24) Kanafani, Z. A.; Perfect, J. R. *Clin. Infect. Dis.* **2008**, *46* (1), 120–128.

(25) Sanglard, D. *Curr. Opin. Microbiol.* **2002**, *5* (4), 379–385.

(26) Rostovtsev, V. V.; Green, L. G.; Fokin, V. V.; Sharpless, K. B. *Angew. Chemie - Int. Ed.* **2002**, *41* (14), 2596–2599.

(27) Tornøe, C. W.; Christensen, C.; Meldal, M. *J. Org. Chem.* **2002**, *67* (9), 3057–3064.

(28) Boren, B. C.; Narayan, S.; Rasmussen, L. K.; Zhang, L.; Zhao, H.; Lin, Z.; Jia, G.; Fokin, V. V. *J. Am. Chem. Soc.* **2008**, *130*, 8923–8930.

(29) Kolb, H. C.; Finn, M. G.; Sharpless, K. B. *Angew. Chemie - Int. Ed.* **2001**, *40* (11), 2004–2021.

(30) Worrell, B. T.; Malik, J. A.; Fokin, V. V. *Science (80-.).* **2013**, *340* (6131), 457–460.

(31) Sagatova, A. A.; Keniya, M. V.; Wilson, R. K.; Monk, B. C.; Tyndall, J. D. A. *Antimicrob. Agents Chemother.* **2015**, *59* (8), 4982–4989.

(32) Sheng, C.; Miao, Z.; Ji, H.; Yao, J.; Wang, W.; Che, X.; Dong, G.; L??, J.; Guo, W.; Zhang, W. *Antimicrob. Agents Chemother.* **2009**, *53* (8), 3487–3495.

(33) Zhou, L.; Amer, A.; Korn, M.; Burda, R.; Balzarini, J.; De Clercq, E.; Kern, E. R.; Torrence, P. F. *Antivir. Chem. Chemother.* **2005**, *16* (6), 375–383.

(34) Weiss, J. T.; Dawson, J. C.; Macleod, K. G.; Rybski, W.; Fraser, C.; Torres-Sánchez, C.; Patton, E. E.; Bradley, M.; Carragher, N. O.; Unciti-Broceta, A. *Nat. Commun.* **2014**, *5*, 3277.

(35) Barral, K.; Moorhouse, A. D.; Moses, J. E. *Drug Discov. Today* **2007**, *9* (9), 1809–1811.

(36) Bruckner, R. *Organic Mechanisms*; 2010.

(37) Lansdown, A. B. G. *Biofunctional Text. Ski.* **2006**, *33*, 17–34.

(38) Bradford, S. S.; Cowan, J. a. *Metallodrugs* **2014**, *1* (1), 10–23.

(39) Ray, S.; Mohan, R.; Singh, J. K.; Samantaray, M. K.; Shaikh, M. M.; Panda, D.; Ghosh, P. *J. Am. Chem. Soc.* **2007**, *129* (48), 15042–15053.

(40) Gök, Y.; Akkoç, S.; Erdoğan, H.; Albayrak, S. *J. Enzyme Inhib. Med. Chem.* **2016**, *31* (6), 1322–1327.

(41) Walker, E. M.; Walker, S. M. *Ann. Clin. Lab. Sci.* **2000**, *30* (4), 354–365.

(42) Demuyser, L.; Swinnen, E.; Fiori, A. **2017**, *8* (4), 1–17.

(43) Sadowska-Bartosz, I.; Pączka, A.; Mołoń, M.; Bartosz, G. *FEMS Yeast Res.* **2013**, *13* (8), 820–830.

(44) Rex, J. H.; Alexander, B. D.; Andes, D.; Arthington-Skaggs, B.; Brown, S. D.; Chaturvedi, V.; Ghannoum, M. a.; Espinel-Ingroff, A.; Knapp, C. C.; Ostrosky-Zeichner, L.; Pfaller, M. a.; Sheehan, D. J.; Walsh, T. J. *Reference method for broth dilution antifungal susceptibility testing of yeasts: approved standard - third edition*; 2008; Vol. 28.

(45) Ghannoum, M. A.; Alexander, B. D.; Andes, D.; Brasso, W. D.; Breown, S. D.; Espinel-Ingroff, A.; Fowler, C. L.; Lockhart, S. R.; Meis, J. F.; Ostrosky-Zeichner, L.; Perlin, D. S.; Ryder, N. S.; Williamson, P. R. *Clin. Lab. Stand. Institute, Wayne, PA* **2012**, *32* (17), 1–32.

7. Appendix

7.1. Fluconazole metalation

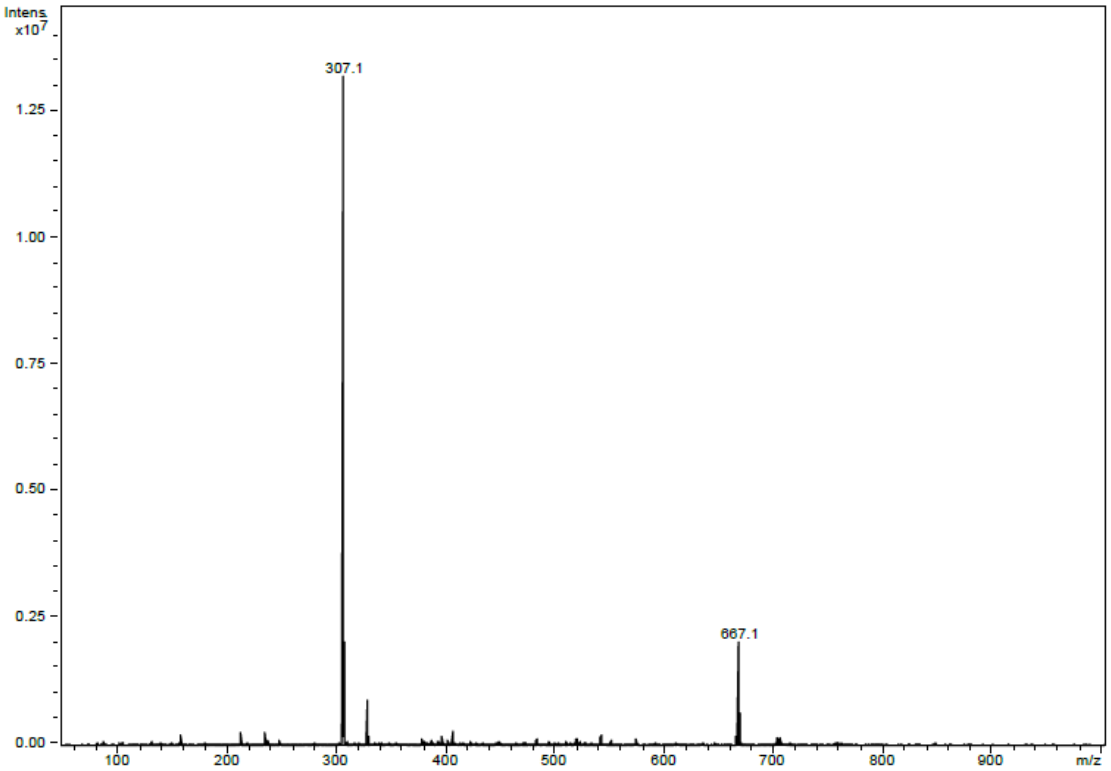

Figure 7.1- Mass spectroscopy spectrum of compound **19**